

# More on Gribov copies and propagators in Landau-gauge Yang-Mills theory

Axel Maas\*

*Department of Theoretical Physics, Institute of Physics,  
Karl-Franzens University Graz, Universitätsplatz 5, A-8010 Graz, Austria and  
Department of Complex Physical Systems, Institute of Physics,  
Slovak Academy of Sciences, Dúbravská cesta 9, SK-845 11 Bratislava, Slovakia*

(Dated: February 6, 2020)

Fixing a gauge in the non-perturbative domain of Yang-Mills theory is a non-trivial problem due to the presence of Gribov copies. In particular, there are different gauges in the non-perturbative regime which all correspond to the same definition of a gauge in the perturbative domain. Gauge-dependent correlation functions may differ in these gauges. Two such gauges are the minimal and absolute Landau gauge, both corresponding to the perturbative Landau gauge. These, and their numerical implementation, are described and discussed in detail.

This investigation is performed, using numerical lattice gauge theory calculations, by comparing the propagators of gluons and ghosts for the minimal Landau gauge and the absolute Landau gauge in  $SU(2)$  Yang-Mills theory. It is found that the propagators are qualitatively different in the far infrared and quantitatively different even at energy scales of the order of half a GeV. In particular, the gluon propagator in minimal Landau gauge seems to be infrared finite while the one in absolute Landau gauge seems to be infrared vanishing in the infinite volume limit, in two and three dimensions. The ghost propagator in absolute Landau gauge is found to be enhanced. Some remarks on the four-dimensional case are provided as well.

PACS numbers: 11.15.Ha 12.38.Aw 14.70.Dj

## I. INTRODUCTION

Green's functions encode the full dynamics of a theory [1]. In gauge theories these are in general gauge-dependent, and it is necessary to determine them in a fixed gauge. In the perturbative regime, this can be conveniently done by local gauge conditions [2]. However, to determine the Green's functions over the full momentum range it is necessary to extend the definition of a gauge into the non-perturbative domain. Unfortunately, there is no unique local possibility to extend the local gauge-fixing conditions of perturbation theory into this regime. One is therefore faced with a, possibly innumerable infinite, number of gauges all corresponding to the same perturbative gauge. This will be further discussed in section II for the example of Landau gauges. In particular, two different Landau gauges will be investigated here in detail, the minimal Landau gauge and the absolute Landau gauge.

The importance of differing non-perturbative completions of perturbative local gauge conditions is that they potentially lead to differences in the gauge-dependent Green's functions. Of course, these differences have to become subleading at sufficiently large momenta, where non-perturbative effects become sub-leading. However, and as will be shown in section IV, these differences may be qualitative at low momenta, and may still be quantitatively relevant at intermediate momenta of the order of the scale  $\Lambda_{YM}$  and above. Hence, not only calculations in the asymptotic infrared momentum range have to take

this into account. Precision calculations of observable quantities, which are based on gauge-dependent correlation functions, may also need to take care of this. Apart from the practical purpose of calculating the Green's functions, this problem is also of a more fundamental interest. Confinement scenarios, like the one of Gribov and Zwanziger [3, 4, 5, 6] and the one of Kugo and Ojima [7] (GZKO), give predictions for correlation functions in certain, well-defined non-perturbative gauges. To check these predictions and hence the scenarios, it is necessary to determine the Green's functions in exactly these gauges.

The determination of the Green's functions is not a trivial problem. To obtain them in the full momentum range, various methods have been employed. Continuum methods, like Dyson-Schwinger equations [8, 9, 10, 11, 12, 13, 14, 15, 16, 17, 18, 19, 20, 21, 22, 23, 24, 25, 26, 27, 28, 29], functional renormalization group equations [16, 30, 31, 32], stochastic quantization approaches [4, 5] or effective action methods [33, 34, 35, 36, 37] have to rely on assumptions, in general. Lattice gauge theory [38, 39, 40, 41, 42, 43, 44, 45, 46, 47, 48, 49, 50, 51, 52, 53, 54, 55] is not in need of such assumptions, but suffers from artifacts, in particular finite volume effects [43, 44, 45, 47, 53, 56]. On top of these problems comes the necessity to fix the same non-perturbative definition of a gauge in all methods. For functional calculations this can possibly be implemented by means of boundary conditions [29]. In case of lattice gauge theory, this is a hard numerical problem, which has been investigated previously [40, 46, 52, 57, 58], and will be discussed in great detail here as well.

Therefore, neither approach alone has been able to provide a final result for the Green's functions. For a reli-

---

\*Electronic address: axel.maas@uni-graz.at

able comparison therefore all of these problems have to be addressed. However, the uncertainties due to the inherent problems in this comparison have sparked quite a prolonged debate on the infrared behavior of Green's functions, and whether they are in agreement with the predictions of the GZKO scenarios or not, for a summary see [29]. In particular, the investigation with lattice calculations has, so far, not yet provided a clear picture. This will be discussed in more detail in section IV, and the issue of gauge fixing on the lattice is covered in section III and appendix B.

In addition to the problem of gauge-fixing, finite volume artifacts are the main problem [43, 44, 45, 47, 53, 56]. The influence of these artifacts has been investigated in detail [43, 44, 45, 47, 53], and seems to indicate a contradiction between the GZKO scenario and the actual form of the Green's functions. However, in these investigations the gauge in the lattice calculation had been different from the one in the continuum. This will be remedied here. Unfortunately, the increase in complexity to fix the same gauge prevents the access of large lattice volumes at the current time in four dimensions. This discrepancy also exists in three dimensions [43, 45, 47], while no discrepancy exists in two dimensions [45, 47, 54]. It is therefore useful to address the problem first in lower dimensions, where large volumes can be accessed more easily. There is another advantage when studying the problem first in lower dimensions: The fixing of the gauge which corresponds to the gauge used in the GZKO scenarios is easier in lower dimensions, as will be shown in section IV.

As a result, it will be shown that the difference between both gauges is in fact the reason for the apparent discrepancy. Once the same gauge as in the GZKO scenario is fixed, the results are also consistent with the GZKO scenario. In particular, the gluon propagator is infrared vanishing and the ghost propagator is infrared enhanced, as will be detailed in section IV. This is the main result presented here.

The organization of the presentation of this result is as follows: In section II, general aspects of fixing Landau gauges in the non-perturbative domain are discussed. Some specific properties of gauge-fixing in connection with Gribov copies are discussed in section III<sup>1</sup>. Afterwards, the direct comparison of the propagators in the minimal and absolute Landau gauge in two and three dimensions is shown in section IV. Some remarks on the four-dimensional case will also be made there. The scenario obtained from these results is discussed in section V. Finally, everything is summed up in section VI. The algorithm to fix (or, at least, approach) the absolute Landau gauge employed here is presented in appendix B.

---

<sup>1</sup> This section is on a technical detail of gauge-fixing procedures in lattice gauge theory. However, it has a certain relevance when the definition of the minimal Landau gauge in the continuum is considered [29].

Technical details of the lattice simulations performed can be found in appendix A.

## II. LANDAU GAUGES IN THE NON-PERTURBATIVE DOMAIN

In perturbation theory, Landau gauge is defined by the local condition

$$\partial_\mu A_\mu^a = 0 \quad (1)$$

on the gauge field  $A_\mu^a$ . It belongs to the class of covariant gauges, which in general average over the (perturbative) gauge orbit with a given weight function [2]. In case of the Landau gauge, this weight function is a  $\delta$ -function. Unfortunately, it has been found [3, 59] that this local condition is insufficient to select a unique representative of the gauge orbit: There are different elements of the gauge orbit, so-called Gribov-Singer copies, which all satisfy the condition (1). An example is, e. g., the instanton [60]. The set of all elements of a gauge orbit satisfying condition (1) will be called the residual gauge orbit. It has been shown that there is no possibility to specify a unique element on the residual gauge orbit with any set of additional local conditions [59].

Further specifications of the gauge will therefore necessarily be non-local. Any of these should reduce to the perturbative Landau gauge (1) in the perturbative limit. This implies that the residual global color symmetry may not be broken by the gauge fixing, except when this breaking is soft, i. e., vanishes in the perturbative limit. As, however, the Kugo-Ojima scenario [7] is based on an unbroken global color symmetry, the judicious choice is not to break it by the gauge condition.

It has been argued long ago that the gauge-fixing will be complete when the gauge field is further restricted to the first Gribov region [3]. This region is characterized by the semi-positiveness of the Faddeev-Popov operator, which in Landau gauge is given by

$$-\partial_\mu(\delta^{ab}\partial_\mu - gf^{abc}A_\mu^c). \quad (2)$$

Unfortunately, this is insufficient [61]. Hence, it is necessary to further restrict the gauge field. A sufficient possibility is to restrict it to the fundamental modular region [61], which is characterized by the condition that the gauge-fixed field configuration absolutely minimizes

$$\mathcal{F}(A) = -\frac{1}{2dV} \int d^d x A_\mu^a(x) A_\mu^a(x), \quad (3)$$

where  $d$  is the dimensionality and  $V$  is the  $d$ -volume. It can further be shown that also all minima of (3) with (2) positive lie in the first Gribov region [5]. Hence, the fundamental modular region is enclosed in the Gribov region. In fact, both have partly a common boundary [6], on which, e. g., instantons lie [60]. The condition (3) can be rewritten after double Fourier transformation as

$$\mathcal{F}(D) = -\frac{N_g}{2^d \pi^{d/2} \Gamma(1 + \frac{d}{2}) V} \int dpp^{d-1} D_{\mu\mu}^{aa}(p), \quad (4)$$

where  $D_{\mu\nu}^{ab}$  is the gluon propagator and  $N_g$  the number of gluons, 3 for SU(2). Therefore, this condition is equivalent to maximizing the total trace of the gluon propagator on the residual gauge orbit. Unfortunately, this is an extremalization problem in a high (in the continuum infinite) dimensional space. It is therefore NP-hard, similar to spin-glass problems. In particular, the complexity increases exponentially with lattice sites. This is one origin of the problems in gauge fixing in numerical lattice gauge theory calculations.

From these observations, it is possible to design different types of non-perturbative Landau gauges. One is the absolute Landau gauge, defined by finding the absolute minimum of (3). In the spirit of the perturbative Landau gauge, this prescription selects exactly one representative on the residual gauge orbit, the one in the fundamental modular region. A second possibility is to select an arbitrary representative of the residual gauge orbit, which lies inside the first Gribov region. This is the most commonly adopted choice in lattice calculations, and is termed the minimal Landau gauge, see e. g. [62]. Of course, other possibilities exist. One would be to average over the part of the residual gauge orbit which lies in the first Gribov region, yielding a Landau-Feynman-like gauge. Another would be to average over the complete residual gauge orbit. The latter is, however, highly non-trivial, but it should be possible to construct [63]. As the origin of field configuration space, and thus perturbation theory, is included in all these prescriptions, the correct reduction to perturbation theory, in the perturbative limit, is guaranteed.

Most interesting is whether and, if, to which extent results depend on this gauge choice. In particular, minimal Landau gauge is rather simple to implement in lattice simulations [62], although some caveats will be discussed in the next section. On the other hand, absolute Landau gauge is the one for which the predictions of the GZKO scenario are valid, and calculations with functional methods [4, 5, 8, 9, 10, 11, 12, 13, 14, 15, 16, 17, 18, 19, 20, 21, 22, 23, 24, 25, 26, 27, 28, 29, 30] may yield results in the absolute Landau gauge [29]. Hence a comparison of these two gauges is of great interest. Such comparisons have been performed repeatedly in the past in four dimensions [40, 46, 52, 57, 58]. However, the results have been rather mixed, and no final result has been obtained so far, although effects seem likely, in particular in the case of the ghost propagator.

Therefore, fixing to the absolute Landau gauge is desirable. Unfortunately, fixing this gauge becomes exponentially harder with the number of lattice sites. Hence, a natural possibility to assess it is to investigate it in lower dimensions, where everything else applies as well, in particular the state of the results [4, 5, 11, 14, 19, 20, 30, 36, 37, 45, 47, 50, 51, 53, 54, 55]. This will be done here, and it will turn out that this, in fact, is simpler and provides currently much more insight.

It has been argued that for expectation values of operators consisting of a product of a finite number of gluon

field operators the results of the minimal and the absolute Landau gauge should coincide in the continuum and infinite volume limit [4]. This would apply to the gluon propagator, although not to the ghost propagator, which depends inversely on the gluon field. There is yet no indication that this is the case at reachable volumes, and also the results presented here do not support this conjecture. It has been argued that this may be a discretization artifact [64].

It should be noted that, due to the factor  $p^{d-1}$  in the integral (4), the far infrared properties of the gluon propagator are likely irrelevant for the distinction between the minimal and the absolute Landau gauge, as, e. g., an effect at 100 MeV can be compensated by a  $10^{d-1}$ -times smaller effect at 1 GeV momentum: Any difference between the gluon propagators in the two gauges in the far infrared is irrelevant to the distinction of the two gauges. This applies in particular to the value of the gluon propagator at zero momentum, which for a non-divergent gluon propagator is not contributing to the integral. In addition, due to asymptotic freedom the far ultraviolet is again irrelevant for the condition (4).

Furthermore, it should be noted that the statement (4) is true for each configuration individually. The quantity on the right hand side of (4) is the gluon propagator on each individual configuration. Nonetheless, the statement is also true on the average, but the distinction may be, and in fact is, only visible at very high statistics due to the  $p^{d-1}$  factor and a difference in (4) which is found to be of only about 0.3% between the minimal and the absolute Landau gauge: For the results presented here, the maximization condition cannot be checked explicitly for the average gluon propagator due to the statistical noise. It is, of course, ensured for each configuration.

The method to fix the absolute Landau gauge is an evolutionary algorithm, which is detailed in appendix B. Note that similar algorithms have been used previously [65, 66]. The minimal Landau gauge will be fixed by an adaptive stochastic overrelaxation algorithm [55, 62].

### III. GAUGE-FIXING

There are a number of peculiarities when it comes to gauge fixing on the lattice, which have to be taken into account when dealing with Gribov copies. One of them is the fact that the complexity of gauge fixing is highly dependent on the configuration. A measure of the complexity is, e. g., the number of steps an iteration method needs to gauge fix a given configuration to the minimal Landau gauge. It turns out that this number varies by orders of magnitudes between different configurations. On the other hand, the extreme case of very complex configurations is rare. There is a relation to the so-called exceptional configurations [40, 55], and hence the same name will be used. Furthermore, it turns out that the complexity also depends on the initialization of the iterative algorithm, i. e., the first guess for the correct gauge

fixing. It is often possible to reduce the number of necessary sweeps considerably by choosing other initial conditions.

It is therefore tempting to restart the gauge-fixing procedure if the situation is exceptional, or even drop the corresponding configuration altogether, to improve computational efficiency. However, in general two different restarts correspond to two different Gribov copies, which is the observation on which many algorithms to fix to the absolute Landau gauge are based on [40, 52]. This may of course lead to a bias when sampling the residual gauge orbit, if the complexity of fixing the gauge is, e. g., related to the distance to the absolute minimum of (3) along the gauge orbit. That such a bias possibly exists is indicated by the fact that a correlation between the value of the lowest eigenvalue of the Faddeev-Popov operator and the number of gauge fixing sweeps has been observed [55]. The aim in this section is to either support this observation by searching for an impact on other observables as well, or to show that this is not the case. This will be done by performing measurements of observables as a function of the number of gauge-fixing sweeps necessary to fix to the minimal Landau gauge. Note that any of these statements apply only to the system investigated here,  $40^3$  at  $\beta = 4.2$ , and may be different for different systems, although empirically these results seem to be typical.

To investigate this, configurations have been obtained from the Wilson action according to [55] and then gauge-fixed to Landau gauge according to [55]. The details of the configurations are given in table I in appendix A. The gauge-fixing procedure was modified by imposing a limiting number of sweeps  $n_s$ . If during gauge-fixing more than this limit would be necessary, then the gauge-fixing process is restarted with another initialization. The latter was always a randomly chosen gauge transformation. If it was not possible to fix the gauge after twenty restarts, the configuration was dropped, and a new one was generated instead.

The results have been compared to the case without any limitation, but otherwise the same gauge-fixing procedure. In this case, the maximum number of gauge-fixing sweeps observed was  $n_s = 28740$ , while the average number was 1528(55), and the minimum number<sup>2</sup> 401. To quantify the amount of exceptional configurations with respect to the limit  $n_s$  the number of necessary restarts and of dropped configurations<sup>3</sup> are shown in figure 1. It is visible that very extreme configura-

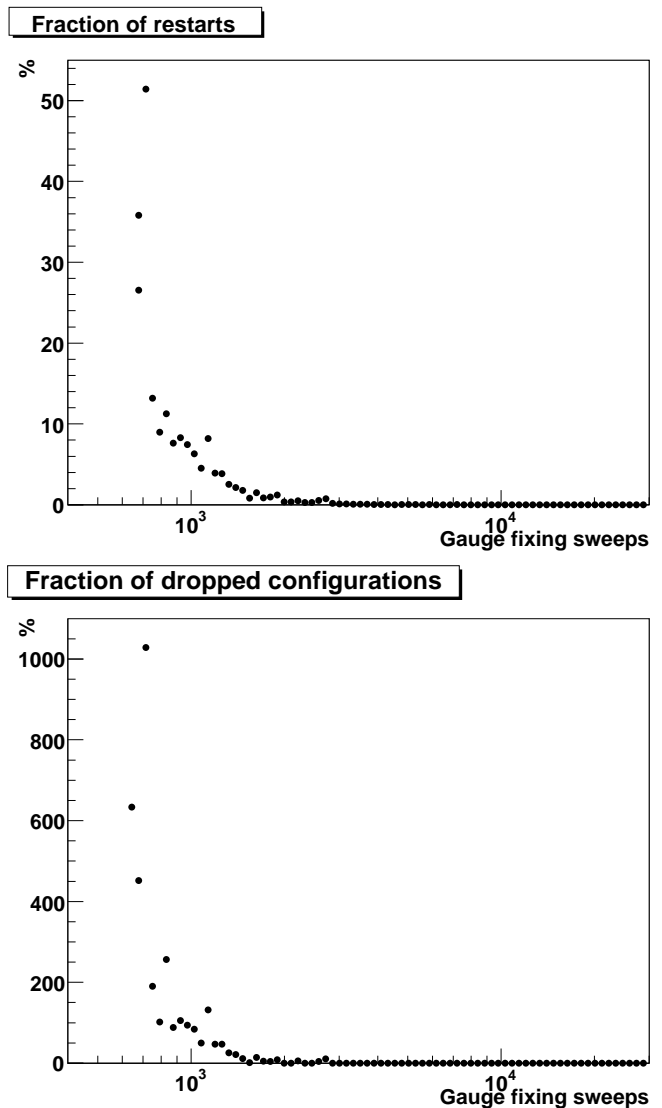


FIG. 1: Top: Fraction of restarts of the maximum possible number of restarts during gauge-fixing as a function of  $n_s$ , not counting dropped configurations. Bottom: Fraction of dropped configurations compared to the total number of configurations as a function of  $n_s$ . Values greater than 100% are possible, if more than every second configuration has been dropped.

<sup>2</sup> This number was due to an optimization of the gauge-fixing procedure, and is actually only an upper limit for the minimum number.

<sup>3</sup> Indications have been found that it is very likely that if one configuration is dropped the next one(s) will be dropped also. This would indicate that the correlation time increases for configurations which are harder to gauge-fix, as the number of sweeps between two gauge-fixed measurements is sufficient for many other observables to decorrelate. To make this a more reliable

statement more investigation is needed, however [67]. To compensate this effect, multiple independent runs have always been performed throughout all results in this paper.

tions are very rare. Within an order of magnitude of the maximum of gauge-fixing sweeps, it was always possible to find another Gribov copy which could be fixed sufficiently fast. Therefore, severe restrictions on the number of gauge-fixing sweeps are necessary for a configurations to be dropped. Still, starting from a certain limit on, a very strong rise in both the number of restarts and the number of dropped configurations is observed.

It turns out that the exceptional configurations have no statistically significant impact on observables as long as the number of restarts is sufficiently small. As an example of the impact on measured quantities, the gluon propagator

$$D_{\mu\nu}^{ab}(x-y) = \langle A_\mu^a(x) A_\nu^b(x) \rangle$$

and the ghost propagator

$$D_G^{ab}(x-y) = - \langle (\partial_\mu (\partial_\mu \delta^{ab} - g f^{abc} A_\mu^c(x)))^{-1} \rangle$$

will be used. In both cases, the color (and, for the gluon propagator, Lorentz) traced<sup>4</sup> and Fourier-transformed propagators will always be shown,  $D(p)$  and  $D_G(p)$ , respectively<sup>5</sup>.

The propagators are shown in figure 2. It is visible that there is essentially no change for the gluon propagator. In case of the ghost propagator the few lowest momentum points are affected, which would be in accordance with the observation of an influence on the lowest eigenvalue of the Faddeev-Popov operator [55]. This latter influence is also observed here, manifesting itself by a systematic increase of the lowest eigenvalue of the Faddeev-Popov operator by about 30%<sup>6</sup>. However, the lowest two momentum points of the ghost propagator are subject to finite volume effects [53, 56], and the consequences are thus less relevant. Thus, at the respective level of biasing the selection of Gribov copies there has almost no consequence within statistical errors for the propagators. As a further observable the gluon propagator at zero momentum will be investigated. This value is particularly important, as will be discussed in the next section. Its dependence on  $n_s$  is shown in figure 3. Again, within statistical errors, there is no consequence of limiting the number of gauge-fixing sweeps.

Therefore, at least for a modest restart policy and at the given level of statistical errors, for the system investigated here, the consequences of the bias observed in [55] have no relevant impact, except for the properties

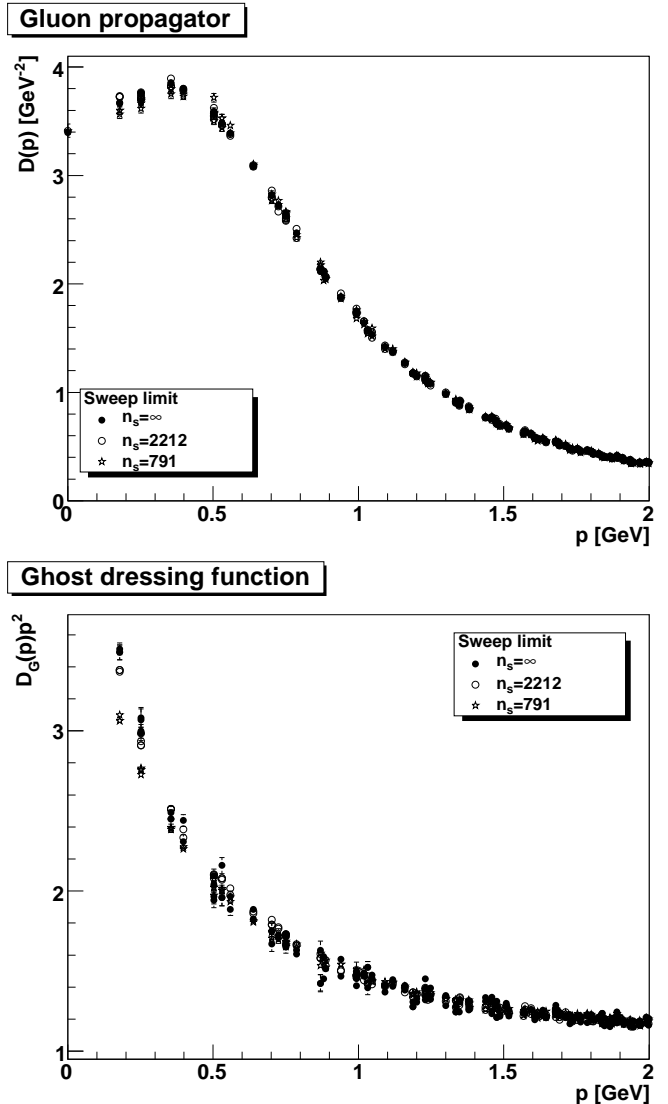


FIG. 2: The gluon propagator (top panel) and the ghost dressing function (bottom panel) as a function of  $n_s$  for  $n_s = \infty$  (full circles),  $n_s = 2212$  (open circles) and  $n_s = 791$  (stars).

of finite volume effects. However, as will be seen in the next section, a bias in selecting Gribov copies can have consequences. Therefore, when desiring to use a limitation to improve the usage of computational resources, it would be necessary to make sure in advance whether for a given system and a given observable this introduces a bias. Hence, no such selection criteria will be used hereafter.

The reason for this effect may be that Gribov copies which are more simple to fix to the Landau gauge are in some sense more 'perturbative', which is by definition almost in Landau gauge. This would also explain the increase of the value of the lowest eigenvalue of the Faddeev-Popov operator. This is also supported by another observation: When the thermalization process is initialized with a cold, i. e. vacuum configuration, and

<sup>4</sup> None of the modifications of the gauge-fixing process performed here or in section IV changes the fact that both propagators are color-diagonal [54, 55].

<sup>5</sup> A more precise definition can be found in [55], along with details on the determination of these quantities, including error determination.

<sup>6</sup> The presented deformation of the sampling procedure of the residual gauge orbit would therefore influence the limits on the infinite volume ghost propagator constructed in [47], if it would be determined with the limits presented here.

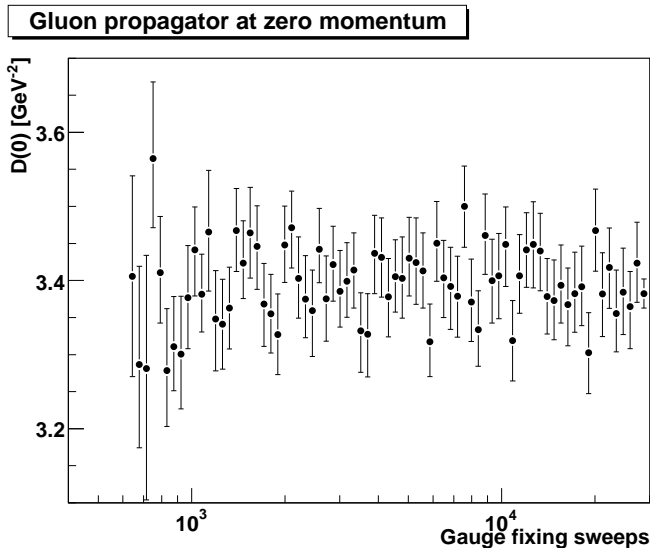


FIG. 3: The gluon propagator at zero momentum as a function of the gauge fixing sweeps limit  $n_s$ .

not enough thermalization sweeps are performed to fully thermalize the configuration, it is usually much simpler to gauge fix than a fully thermalized configuration.

However, as there is an effect on correlation functions by performing this modification of the minimal Landau gauge it implies that 'minimal Landau gauge' is not by itself a sufficiently precise description of the gauge. Implicitly assumed is that dropping configurations is only a convenient numerical simplification, and is not altering the sampling of configurations. This is supported by the fact that the alterations observed have a smooth onset even when none or only a statistically insignificant number of configurations are dropped. A more precise description is hence needed to qualify what is meant by 'choosing randomly one representative inside the first Gribov region'. This has to be understood further to give a precise meaning to the concept of the minimal Landau gauge. Here, as an operational definition of the gauge the description of the gauge-fixing algorithm (with no limit on the number of sweeps) [55] will be used.

#### IV. MINIMAL VS. ABSOLUTE LANDAU GAUGE

In the following the propagators, as examples of gauge-dependent Green's functions, in minimal and absolute Landau gauge will be compared. Aside from the general question to which extent gauge-dependent correlation functions actually differ in the two gauges, there is another reason to pose this question. Predictions exist from functional calculations on the infrared behavior of these correlation functions [4, 8, 11, 17], in fact, for any correlation function [13, 19], in absolute Landau gauge. These predict a power-law behavior of

the correlation-functions in the far infrared, which is, if it exists, unique [16]. In particular, the ghost propagator would be more singular than that of a massless particle, and the gluon propagator would be infrared vanishing if the ghost-gluon vertex were infrared constant [4, 8, 10, 11]. The latter is, inside this scenario, likely [14, 16, 19], and supported by lattice calculations [49, 50, 54]. This applies to two, three and four dimensions. However, as another possibility it has been proposed that the gluon propagator should be infrared finite and the ghost propagator behave like the one of a massless particle. This has been proposed in three and four dimensions [21, 22, 23, 24, 25, 26, 27, 33, 34, 35, 36, 37].

The functional methods generally suffer from necessary assumptions and approximations to make them solvable. Although this necessity has been greatly reduced over time [13, 16, 19, 29], the question which is the infrared behavior of the correlation functions still induces uncertainties. Therefore, it is natural to compare these results to lattice calculations, which have no need for assumptions. On the other hand, they suffer from artifacts due to finite volumes, discretization and numerical requirements. In particular, finite volumes have been a serious issue, especially in four dimensions [53]. Recently, however, computational resources have become available, which reduced this problem considerable, at least for Yang-Mills theory with sufficiently coarse discretization [43, 44, 45, 47].

A serious obstacle is still the necessity to fix to the absolute Landau gauge. This is a minimization problem in a high-dimensional space, therefore NP-complete, and thus exponentially hard. However, arguments have been made that at least for the gluon propagator in the limit of infinite volume in the continuum the results should be identical in the minimal and the absolute Landau gauge [4]. Therefore, the numerically much simpler, since polynomially hard, minimal Landau gauge has been used to obtain results for the propagators on the lattice. These are in good agreement with an infrared finite gluon propagator and a massless ghost propagator in four and three dimensions [43, 44, 45, 47], but an infrared vanishing gluon propagator and infrared enhanced ghost propagator in two dimensions [45, 47, 54].

Still, the claim that both gauges coincide on the level of propagators has to be verified. Various attempts have been made, all on (necessarily) small volumes in four dimensions [40, 46, 52, 57, 58]. Some discrepancies have been found for the ghost propagator between both gauges, which may or may not decrease with volume. However, as the problem increases with the dimensionality of the space, and thus lattice sites, it can be expected that it is much simpler in lower dimensions. Furthermore, it has been found that in two dimensions the results are clearly in favor of a power-law solution [54]. It is therefore suggestive that also in higher dimensions in fact the power law solution would persist in the absolute Landau gauge. This is supported by the fact that in three dimensions, where the problem should be more severe than in two but less than in four, at least partly a power-law so-

lution is observed [51], and a discrepancy only appears at very large volumes [45, 47]. It is therefore a natural investigation to check the situation in two and three dimensions. This will be done here.

To this end, an evolutionary algorithm [68] will be used, which is described in detail in appendix B. Still, this algorithm is not able to guarantee to fix to the absolute Landau gauge, as it cannot guarantee to find the absolute minimum of the gauge-fixing functional (3). This is a general problem [40, 46, 52, 57, 58, 65, 66] for this type of minimization problems, which belongs to the same class as finding the ground state energy of spin-glass models. Only in the asymptotic limit of infinite computing time success can be guaranteed.

This has the unpleasant consequence that, even if the algorithm actually succeeded in finding the absolute minimum, it would be impossible to tell so. The only thing which can be hoped for is that the found gauge-fixed configuration is 'closer' to the absolute Landau gauge. Even a notion of 'closer' is impossible to define rigorously, as it is even unknown whether any type of gauge-fixing of the residual gauge orbit is smoothly connected to the absolute Landau gauge or not. That this is the case will be assumed henceforth.

Therefore, as a pragmatic ansatz, the fulfillment of the condition (4), finding the gluon propagator with the maximum total trace, will be taken as a criterion to compare the closeness to the absolute Landau gauge of two gauge-fixed configurations. Hence, the gauge-fixed configuration with the least value of  $\mathcal{F}(A)$  found will be taken to be in the absolute Landau gauge. In addition, as a measure of the presence of Gribov copies the difference

$$\Delta = \mathcal{F}(A_{\text{worst}}) - \mathcal{F}(A_{\text{best}}) \quad (5)$$

will be used, where 'best' and 'worst' refer to the gauge-fixed field for a given configuration having the lowest and highest value of  $\mathcal{F}(A)$ , respectively.

It turns out that the function (5) has a generic shape, with potentially three, rather sharp, peaks. The lowest has values of  $\Delta$  of the order of the numerical precision, and is therefore clearly due to numerical noise. The second peak clusters at very small values, typical of around the order of  $10^{-15}$ , likely due to lattice Gribov copies [69]. The third peak is around  $10^{-3}$  and appears to be related to continuum Gribov copies. With increasing volume, the population moves from the lowest to the highest peak. At sufficiently large volumes, only the peak at the highest value of  $\Delta$  is populated. This could indicate that then at least one continuum Gribov copy is present in each configuration, in addition to any lattice copies.

Technical details on the lattice simulations performed can be found in appendix A.

### A. Two Dimensions

The case of two dimensions is particularly interesting, as the results in lattice calculations and in continuum

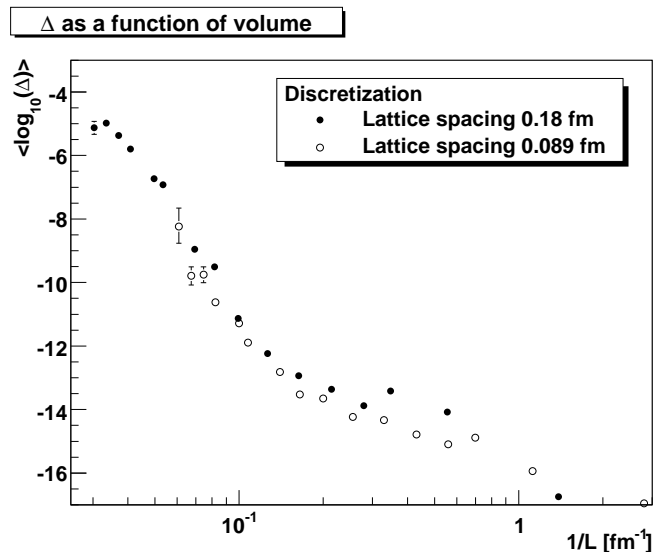


FIG. 4: The presence of Gribov copies as measured by  $\Delta$  as a function of inverse volume in two dimensions. Full circles correspond to  $\beta = 10$ , while open circles correspond to  $\beta = 38.7$ .

functional calculations agree [5, 54]. Furthermore, in this case the finite-volume effects for the gluon propagator behave in exactly the same way as in functional calculations, while they are apparently different for the ghost propagator [54, 56]. It is therefore highly interesting, whether a difference in terms of correlation functions between the minimal and absolute Landau gauge exists, and, in particular, whether this will harm the agreement between the continuum and the lattice results.

The dependence of  $\Delta$  on the (inverse) volume is shown in figure 4. Even at quite large volumes,  $\Delta$  is still rather small, implying that a considerable amount of the configurations do not yet turn up in the peak with the highest value of  $\Delta$ . This would indicate that in many cases the difference between the best and the worst Gribov copy is still negligible in terms of the gluon fields themselves. On the other hand, the exponential rise with volume is still clearly visible. It cannot, however, be anticipated at which level the function finally levels, and thus, whether Gribov copies could have a sizeable impact on the gluon fields at sufficiently large volumes. This remains to be seen. Furthermore, the discretization has only a small effect. In addition, this effect decreases with increasing volume.

However, a statement on the average difference between the field variables is not sufficient for a statement on their correlation functions. Therefore, these are studied separately. For a very large volume, the difference between the propagators in minimal Landau gauge and in absolute Landau gauge are shown in figure 5. The impact is quantitatively rather small for the propagators in the two different gauges. A statistically significant effect is only seen for the ghost propagator at momenta below

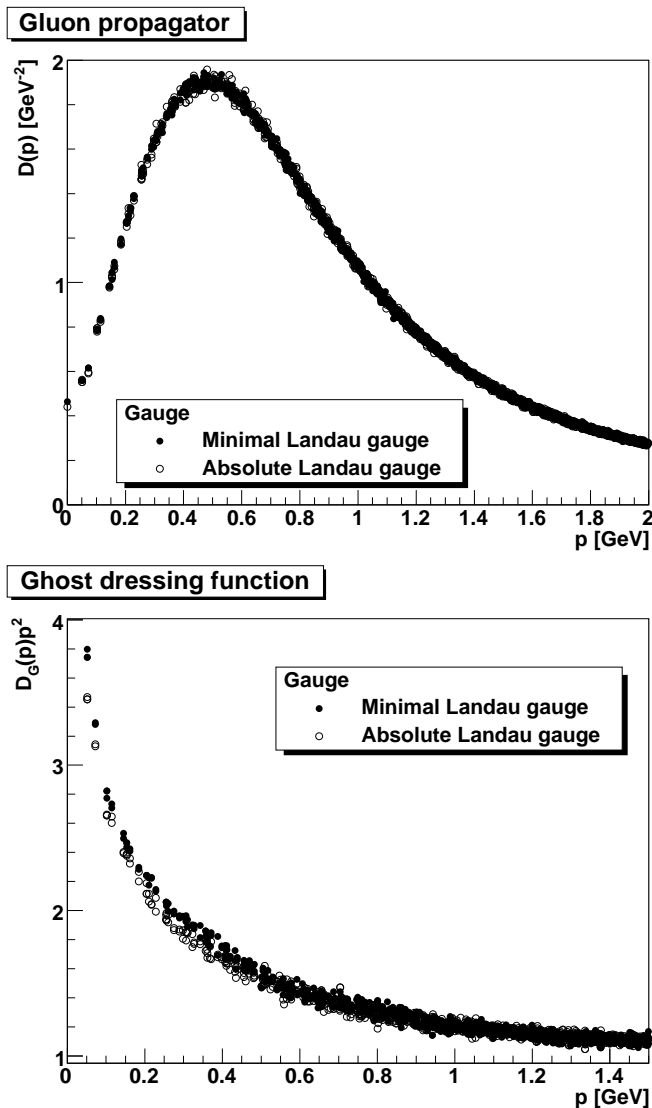


FIG. 5: The propagators from a  $136^2$  ( $(25 \text{ fm})^2$ ) lattice at  $\beta = 10$ . The top panel shows the gluon propagator and the bottom panel the ghost dressing function. Full circles correspond to the results in the minimal Landau gauge and open circles to the absolute Landau gauge.

250 MeV. There, the propagator in the absolute Landau gauge is systematically smaller than in minimal Landau gauge. However, the effect is strongest for the two lowest momentum points, which are anyhow unreliable due to finite volume effects. There is also a small effect on the border of statistical significance for the gluon propagator. The gluon propagator in absolute Landau gauge is smaller in the infrared than the one in minimal Landau gauge. This requires a compensation at larger momenta by virtue of the condition (4), which is too small to be seen due to the statistical fluctuations. Nonetheless, the strongest effects are in the domain where finite volume artifacts dominate. Therefore, the effect is almost negligible. Still, the volume dependence of the gluon propaga-

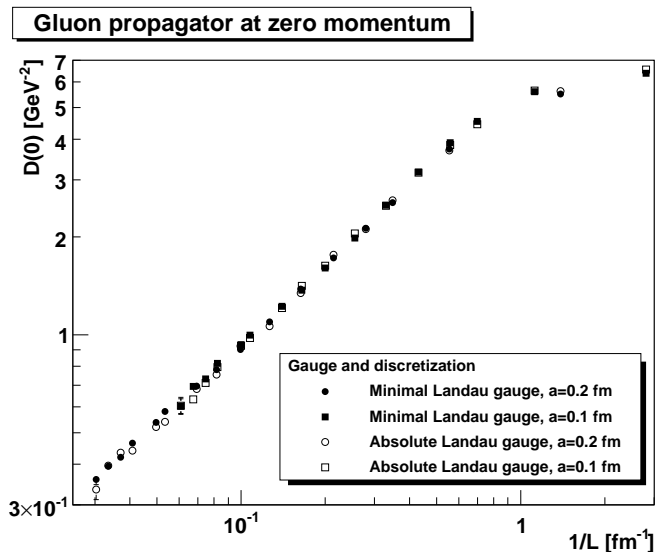


FIG. 6: The gluon propagator at zero momentum as a function of inverse volume. Full and open symbols correspond to the minimal and absolute Landau gauge, respectively. Circles are from calculations at  $\beta = 10$  and squares from calculations at  $\beta = 38.7$ .

tor at zero momentum is a quantity for which predictions exist [56], and which in the minimal Landau gauge are fulfilled [54]. In particular, it behaves as a power-law and vanishes in the infinite-volume limit. This is not altered in the absolute Landau gauge, as seen in figure 6. As can be seen, there is essentially no difference in the volume dependence, and both are in agreement with the predictions from functional calculations.

A final possibility for comparison are differential characteristics of the propagators. Both propagators are predicted to behave as power-laws in the far infrared region [5, 11]. This can be parameterized by

$$D(p) \approx_{p \ll \Lambda_{\text{YM}}} A_Z (p^2)^{-1-t}$$

$$D_G(p) \approx_{p \ll \Lambda_{\text{YM}}} A_G (p^2)^{-1-\kappa},$$

with constant prefactors  $A_Z$  and  $A_G$ . In particular, the effective infrared exponents  $t$  and  $\kappa$  as a function of volume are interesting, as they are the key quantities in comparison to functional calculations. This volume dependence of the exponents, determined in the same manner as in [54], is shown in figure 7. The gluon exponent  $t$  does not differ in both gauges, and in both cases it tends towards the predicted value in the infinite volume limit. In case of the ghost exponent, there seems to be a systematic difference, both in central value and in volume dependence between both gauges. However, this fact is not statistically significant<sup>7</sup>. In addition, in both gauges

<sup>7</sup> With the statistics employed in [54], this difference would not have been visible at all.

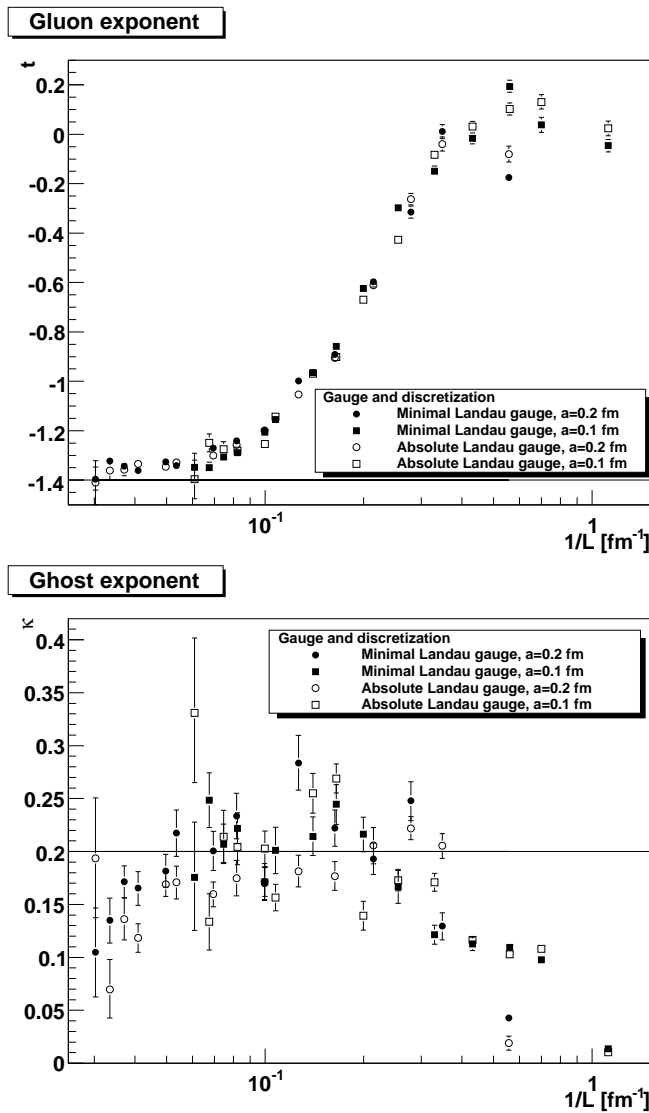


FIG. 7: The gluon exponent  $t$  (top panel) and the ghost exponent  $\kappa$  (bottom panel) as a function of volume. Full and open symbols correspond to the minimal and absolute Landau gauge, respectively. Circles are from calculations at  $\beta = 10$  and squares from calculations at  $\beta = 38.7$ . The lines indicate the infinite-volume predictions from functional calculations [5].

the exponent is compatible to the predicted value, within statistical accuracy. The variations of the central values for the two largest volumes indicate that the results at the respective level of statistics become already unreliable, a consequence of the fit procedure [54].

A more sensitive test is the relation predicted between both exponents [5, 8, 11, 30]

$$t = -2\kappa - \frac{4-d}{2}. \quad (6)$$

As a consequence, the quantity

$$\alpha(p) = D(p)D_G(p)^2 p^{2+d} \quad (7)$$

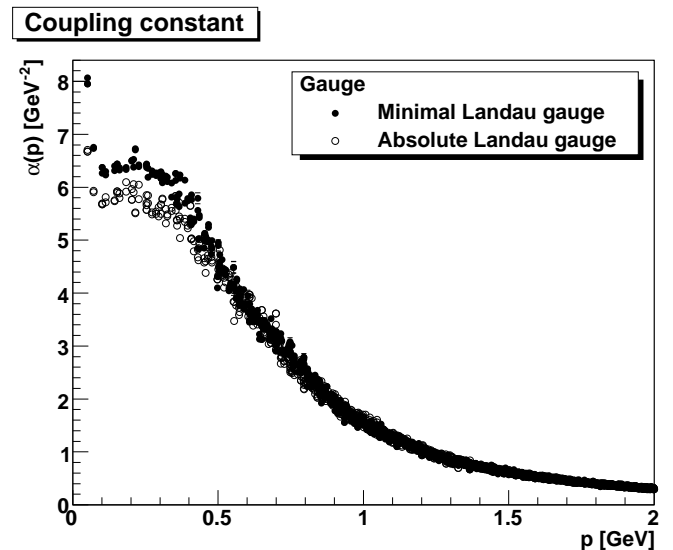


FIG. 8: The quantity (7) from a  $136^2$  ( $(25 \text{ fm})^2$ ) lattice at  $\beta = 10$ . Full circles correspond to the results in the minimal Landau gauge and open circles to the absolute Landau gauge. Note that the two lowest momentum points are affected by finite volume artifacts [54].

should be a constant in the far infrared. This quantity is proportional to a possible definition of the coupling constant [11] and can be regarded as an effective coupling constant.

The relation (6) holds in both gauges, as can be seen from the quantity (7) shown in figure 8. However, the constant of proportionality shows a difference between both gauges. This implies that the difference observed for the ghost propagator in both gauges in figure 5 is likely rather due to a change in the prefactor  $A_G$  from gauge to gauge than in the value of the exponent  $\kappa$ .

Hence, it seems that there is at best a quantitative difference between the propagators in both gauges, but not a qualitative one. Even this quantitative difference seems to be rather small. In particular, the propagators in both gauges agree with the predictions from functional calculations in the continuum. However, after investigating the case in three dimensions in the next section, it will be necessary to reconsider this conclusion. This will be done in section V.

## B. Three Dimensions

In three dimensions, the situation is quite different than in two dimensions. The predictions from functional calculations are qualitatively identical [5, 11, 20, 30]. Results on small and medium-sized lattices seem to confirm these predictions [51, 55, 70]. However, results on the largest lattices suggest rather an infrared finite gluon propagator and an infrared tree-level-like ghost propagator [45, 47]. Still, in an intermediate momentum window

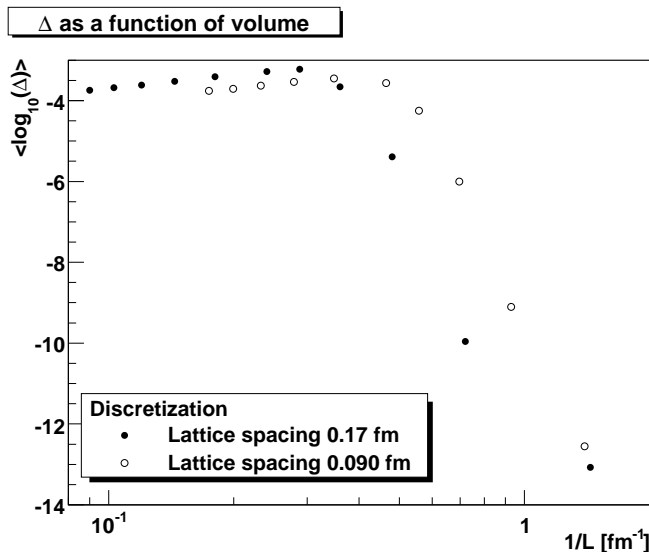


FIG. 9: The presence of Gribov copies as measured by  $\Delta$  as a function of inverse volume in three dimensions. Full circles correspond to  $\beta = 4.24$ , while open circles correspond to  $\beta = 7.09$ .

these results exhibit, at least qualitatively, the behavior predicted in functional calculations [20, 55]. The latter observation is not a finite volume effect.

Starting again with the measure for the presence of Gribov copies  $\Delta$ , the result is already drastically different from the two-dimensional case. This is shown in figure 9. As in the two-dimensional case, an exponential rise with volume is visible. However, it saturates at a value of about  $10^{-3}$ , corresponding to the highest-valued peak in the distribution of  $\Delta$ . In fact, at the largest volumes,  $\Delta$  is confined to a rather small region around this peak, implying that in all configurations there are significant differences in terms of  $\mathcal{F}(A)$  between the best and worst Gribov copy. If these large differences in fact correspond to continuum Gribov copies, this implies that, starting from volumes of the order of about  $(3 \text{ fm})^3$ , Gribov copies play an important role.

A little detail is that  $\Delta$  seems to decrease once more when the volume becomes larger. This is more drastically seen when averaging  $\Delta$  on a linear scale, as shown in figure 10. Here, it is visible that  $\Delta$  starts to decay significantly with increasing volume. On the one hand, this can indicate that the local minima become more and more degenerate with the absolute minimum, and is thus a statement on the nature of Gribov copies<sup>8</sup>. It could also imply that the gauge-fixing algorithm becomes unable to find a good approximation of the absolute minimum. This would be possible if the search space covered is not

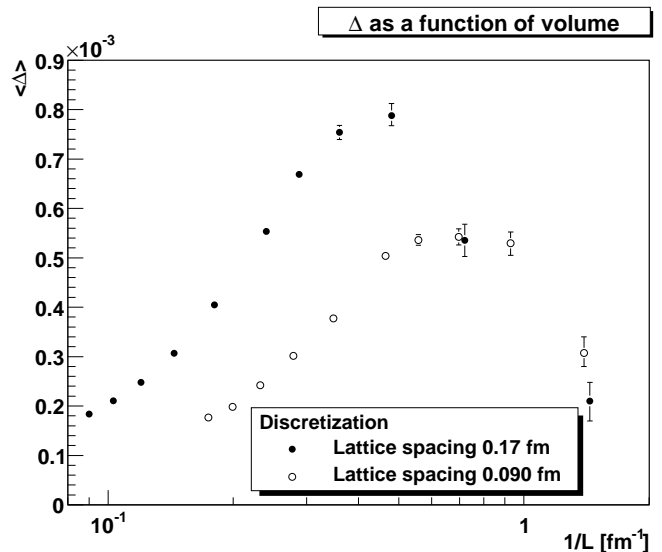


FIG. 10: The presence of Gribov copies as measured by  $\Delta$  as a function of inverse volume in three dimensions, averaged on a linear scale. Full circles correspond to  $\beta = 4.24$ , while open circles correspond to  $\beta = 7.09$ .

sufficiently enlarged to compensate for the exponential increase of the number of Gribov copies with volume. This possibility is discussed in more detail in appendix B. It could, of course, also be a mixture of both effects. Anyway, it may potentially be affecting the reliability of the results at sufficiently large volumes. Eventually, if the computational resources are not increased exponentially with volume as well, the gauge-fixing algorithm will fail. As a consequence, the result will become indistinguishable from the ones in minimal Landau gauge. This may be the onset of it. A third possibility is that the Zwanziger conjecture may be correct in the end: A decrease in  $\Delta$  implies that the integrated strength of the gluon propagator becomes more and more similar between minimal and absolute Landau gauge once more, leading possibly eventually to coinciding gluon propagators. However, it will be shown below that this is not equivalent to a point-wise coincidence of the gluon propagators yet, although some degradation is observed for the results in the largest volume.

Monitoring the gluon propagator is another possibility to measure the success of the gauge-fixing procedure. The result for the gluon propagator in both gauges is shown in one large volume in figure 11. Alongside also the volume dependence of the propagator in the infrared and the behavior of it at zero momentum are shown. First of all, the statistically significant difference is quantitatively rather small, and confined to momenta below roughly half a GeV. The latter is expected, as the difference between both gauges is purely non-perturbative, and should therefore decrease as a power of momentum towards large momenta, leaving only the identical perturbative part of the propagators.

<sup>8</sup> This happens, e. g., in 2d  $U(1)$  gauge theory [71]. I am grateful to L. von Smekal for pointing out this possibility.

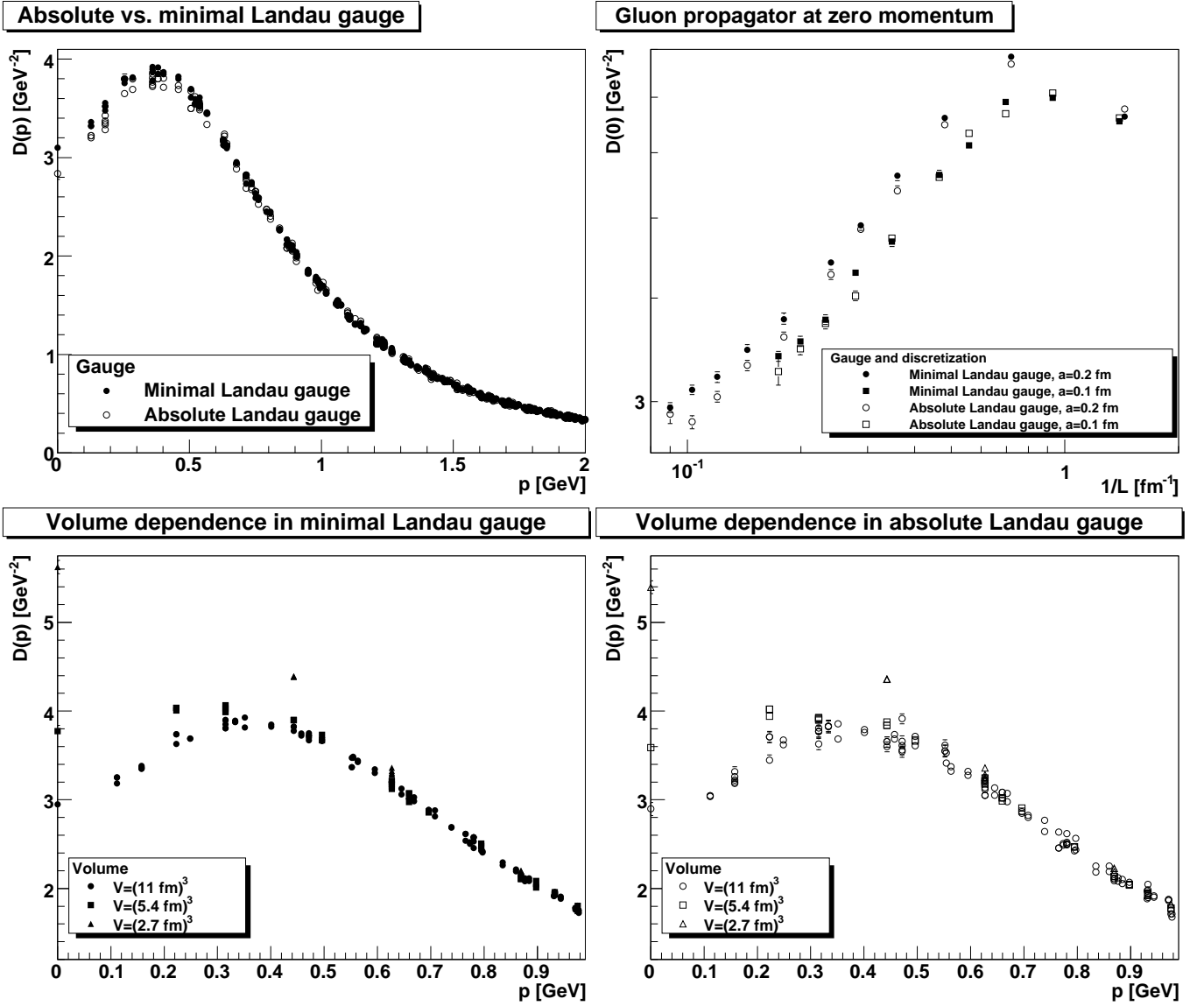


FIG. 11: The gluon propagator in three dimensions. The top left panel shows the comparison between minimal (full circles) and absolute (open circles) Landau gauge on a  $56^3$  lattice at  $\beta = 4.24$ , corresponding to  $V = (9.5 \text{ fm})^3$ . The bottom panels show the volume dependence for the gluon propagator in minimal (left panel) and absolute (right panel) Landau gauge. Circles, squares, and triangles correspond to  $V = (11 \text{ fm})^3$ ,  $(5.4 \text{ fm})^3$ , and  $(2.7 \text{ fm})^3$ , respectively, all calculated at  $\beta = 4.24$ . The top right panel shows the gluon propagator at zero momentum. Full symbols are from the minimal Landau gauge, while open symbols are from the absolute Landau gauge. Circles and squares correspond to calculations at  $\beta = 4.24$  and  $\beta = 7.09$ .

Interestingly, the statistically significant deviations lead to a gluon propagator which is smaller at low momenta than the one in minimal Landau gauge, contrary to the condition (4). As, on each configuration individually, the condition (4) is nonetheless fulfilled, this implies that the propagator in absolute Landau gauge will be larger than the one in minimal Landau gauge in some intermediate momentum range. However, as discussed

above, this is not visible due to the statistical noise<sup>9</sup>.

Hence, the gluon propagator in absolute Landau gauge is more strongly infrared suppressed than in minimal Landau gauge. In particular, the gluon propagator at zero momentum decays faster in absolute Landau gauge

<sup>9</sup> Note that the results for both gauges are obtained from two independent sets of configurations to reduce systematic errors. Hence a direct configuration-by-configuration comparison is not possible. Furthermore, fulfillment of the condition (4) may be implemented at different momenta for different configurations.

than in minimal Landau gauge, and continues longer in a power-law decay towards the infinite-volume limit, while in minimal Landau gauge the gluon propagator seems to exhibit a mass-like behavior, as has been observed previously [43, 45]. Only for the largest volume the value of the propagator at zero momentum seems to rise once more. However, as there is no similar effect for non-zero momentum, and the statistical error is comparatively large, this may, or may not, be a statistical fluctuation. Otherwise, it may be an effect due to the one observed in figure 10 that  $\Delta$  decreases for large volumes. Beyond this, at least for the volumes investigated here, this decrease does not (yet) have an effect. In general, the gluon propagator in absolute Landau gauge therefore seems to behave as predicted in the GZKO scenario, and vanishes at zero momentum in an infinite volume. In minimal Landau gauge, however, it seems to develop a mass, and becomes infrared constant. Furthermore, both behave similarly but not the same as a function of volume: The one in absolute Landau gauge follows the predicted pattern [56] in the GZKO scenario.

Corresponding results for the ghost propagator are shown in figure 12. The results are highly interesting. Comparing within a small volume the propagator in both gauges, it is found that the one in absolute Landau gauge is significantly smaller up to momenta as large as nearly 1 GeV than the one in minimal Landau gauge. In a larger volume, however, both look much more similar again. The reason for this behavior can be seen from the volume-dependence of the propagator in both gauges. In minimal Landau gauge, the propagator becomes less and less infrared enhanced with increasing volume, until it eventually becomes essentially the one of a massless particle [43, 47]. This is, however, not the case in the absolute Landau gauge. While it also becomes less divergent for small volumes, the situation changes when Gribov copies become relevant. Then, the propagator stays at least as divergent as it was on smaller volumes, or may possibly become even more divergent again. With, admittedly, an overly optimistic interpretation, the residual finite-volume effects for the lowest momentum point may even be the same as those predicted in the GZKO framework [56].

These results are reflected also in the spectrum of the Faddeev-Popov operator, in particular on its lowest eigenvalue. However, the statistical uncertainty in this case is too large for a definite conclusion.

To complete the collection of results on the propagators, two more properties are investigated. One is again the differential properties in the form of the effective exponents  $t$  and  $\kappa$ , which are shown in figure 13. The exponent for the gluon propagator is mildly affected at large volumes, becoming more negative in the absolute Landau gauge. Still, the volume is such that also in minimal Landau gauge the exponent is smaller than  $-1$ , but larger than the one in absolute Landau gauge. Both are in accordance with an infrared vanishing gluon propagator. In case of the ghost exponent, the difference be-

tween both gauges is more pronounced, but statistical uncertainties prevent a definite conclusion at large volumes. In particular, as can already be deduced from the ghost dressing function in figure 12, the ghost exponent is initially larger in minimal Landau gauge than in absolute Landau gauge. The exponent in minimal Landau gauge, however, decreases with volume [43, 47] while the one in the absolute Landau gauge is essentially volume independent within statistical accuracy. This once more demonstrates that the results in absolute Landau gauge approach the ones of the GZKO scenario.

Finally, the quantity  $\alpha$ , defined in equation (7), should become constant for all dimensions in the far infrared, and thus also in three dimensions. This is the case in two dimensions in both gauges, as shown above. However, it seems to go to zero in three and higher dimensions [43]. However, this is to be expected in any finite volume [56], but the pattern of finite volume artifacts observed in minimal Landau gauge is not in agreement with a constant value in the infinite volume limit [45, 47]. The result in absolute Landau gauge, and its volume dependence, is shown in figure 14. The difference between both gauges is not qualitative, in particular, in both cases  $\alpha$  seems to go to zero. However, there is an interesting volume dependence observed in the absolute Landau gauge. It is seen that with increasing volume the maximum tends to move towards smaller momenta, albeit rather slowly. The consequence of this is particularly visible in case of the lowest momentum point: The same value of  $\alpha$  is attained at smaller and smaller momenta on the decreasing slope. This would be in accordance with the type of finite volume effects predicted in the GZKO scenario [56]. Hence, this could be regarded as support for the prediction of relations between the exponents (6) of the correlation functions in the far infrared, like the one forcing  $\alpha$  to be constant in the infrared.

### C. A note on four dimensions

Take now for a moment for granted that in absolute Landau gauge the GZKO scenario along with all predictions is correct. This would imply that the effective gluon exponent would become smaller with increasing dimension, while the one for the ghost becomes larger [5]. Given the volumes from which onward a maximum in the gluon propagator can be observed in two and three dimensions, it can be immediately deduced that lattice volumes of the order of  $50^4$  at  $\beta = 2.2$  would be necessary to obtain such a maximum unambiguously in four dimensions. Furthermore, from the results for  $\Delta$  obtained on small lattices, which is shown in figure 15 and should be compared to the figures 4 and 9, it is clear that the number of Gribov copies in four dimensions at a given linear lattice extension in lattice units significantly exceeds the same number in lower dimensions. As assured in the beginning the issue of Gribov copies becomes more severe with an increasing number of dimensions.

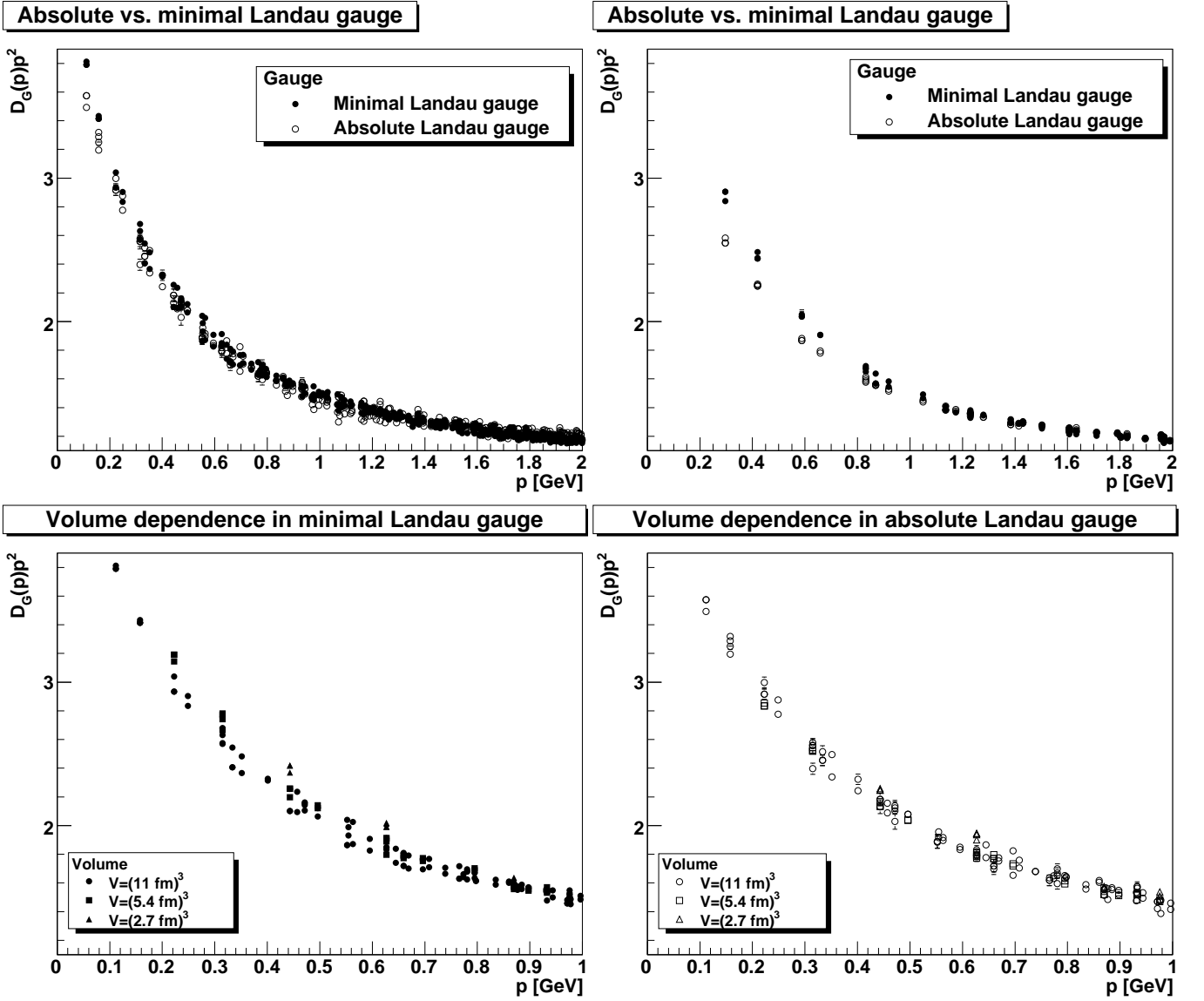


FIG. 12: The ghost dressing function in three dimensions. The top left panel shows the comparison between minimal (full circles) and absolute (open circles) Landau gauge on a  $64^3$  lattice at  $\beta = 4.24$ , corresponding to  $V = (12 \text{ fm})^3$ , the right panel shows the same comparison for a  $24^3$  lattice, corresponding to  $V = (4.1 \text{ fm})^3$ . The bottom panels show the volume dependence for the ghost dressing function in minimal (left panel) and absolute (right panel) Landau gauge. Circles, squares, and triangles correspond to  $V = (11 \text{ fm})^3$ ,  $(5.4 \text{ fm})^3$ , and  $(2.7 \text{ fm})^3$ , respectively, all calculated at  $\beta = 4.24$ .

From this already a rough estimate of the necessary computing time can be deduced, which will be needed to obtain the propagators in absolute Landau gauge for the indicated volume. This exceeds the amount of computing time invested here for the the calculations in two and three dimensions by more than an order of magnitude. Aside from this, the necessary amount of storage space at intermediate steps of the calculations to hold all the gauge transformations needed in parallel for the algorithm presented in appendix B is also rather prohibitive. Hence, this has to be investigated in detail further, when sufficient resources will be available in the near future.

## V. DISCUSSION

The results found suggest that in the absolute Landau gauge indeed the propagators behave like power-laws in the far infrared, in both two and three dimensions. On the other hand, in the minimal Landau gauge they seem to exhibit a massive pattern, in agreement with [43, 44, 45, 47]. In particular, given the results for  $\Delta$  in two dimensions in figure 4 in comparison with the ones in three dimensions shown in figure 9, it is likely that for sufficiently large volumes the propagators in the minimal Landau gauge will exhibit a massive behavior also in

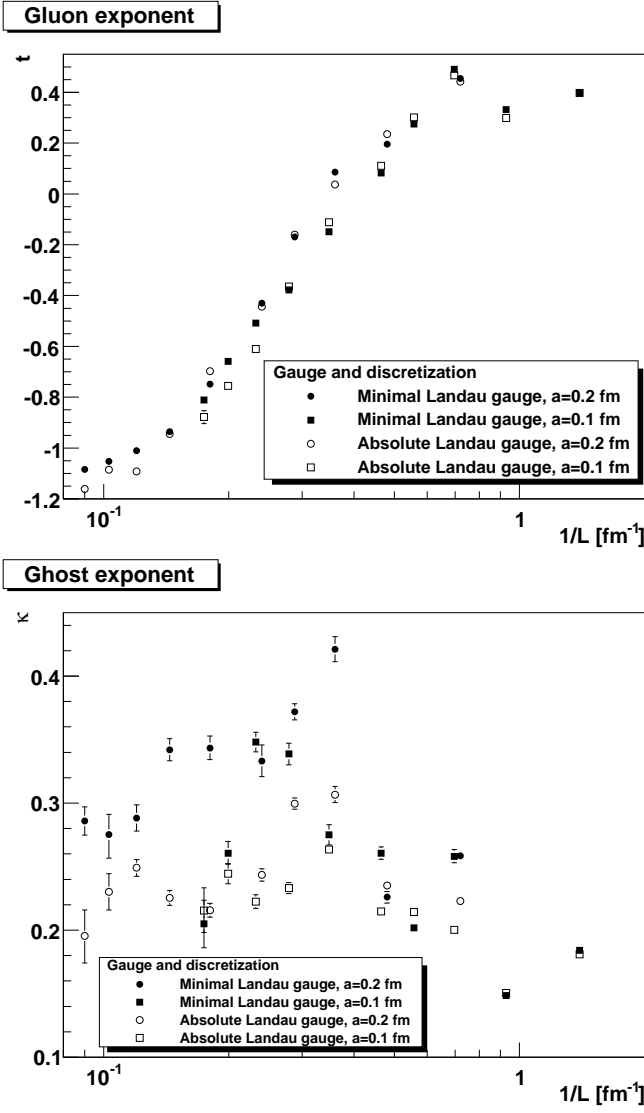


FIG. 13: The gluon exponent  $t$  (top panel) and the ghost exponent  $\kappa$  (bottom panel) as a function of volume in three dimensions. Full and open symbols correspond to the minimal and absolute Landau gauge, respectively. Circles are from calculations at  $\beta = 4.24$  and squares from calculations at  $\beta = 7.09$ .

two dimensions. But for the volumes investigated so far this is not yet the case, and the difference between both gauges in terms of the propagators remains negligible. Furthermore, for sufficiently large volumes in any dimension the amount of Gribov copies will become so large that with the available resources it will not be possible to obtain results in the absolute Landau gauge. Therefore, even when employing algorithms like the one used here, also in this gauge the propagators will not remain power-laws. This is then a pure artifact when not supplying computing time increasing exponentially with volume as well. Furthermore, sufficient numerical precision will be needed, if local minima become nearly degenerate

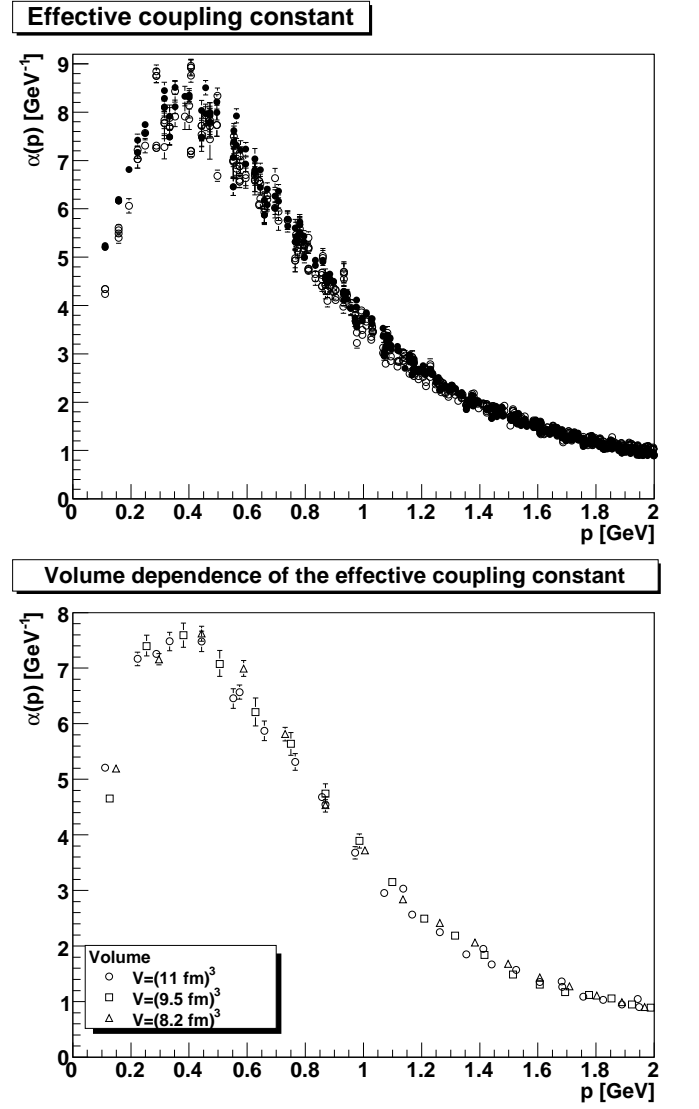


FIG. 14: In the top panel the quantity  $\alpha$ , defined in (7) is shown in minimal Landau gauge (full circles) and in absolute Landau gauge (open circles). In the lower panel the volume dependence of the effective coupling constant in absolute Landau gauge is shown. Circles are from a  $64^3$  lattice, squares from a  $56^3$  lattice, and triangles from a  $48^3$  lattice, all calculated at  $\beta = 4.24$ .

with the absolute one.

Viewed from a more optimistic perspective, the results support that the Gribov problem becomes more severe with increasing dimensionality. Therefore it is highly probable that even in four dimensions, resources granted, a power-law behavior will be observed in the propagators. Especially the fact that numerous other quantities show a smooth behavior as a function of dimension in Yang-Mills theory makes this conjecture likely.

In addition, the effects are quantitatively rather small for the volumes investigated here, and it is mostly the volume dependence which is affected. It therefore seems

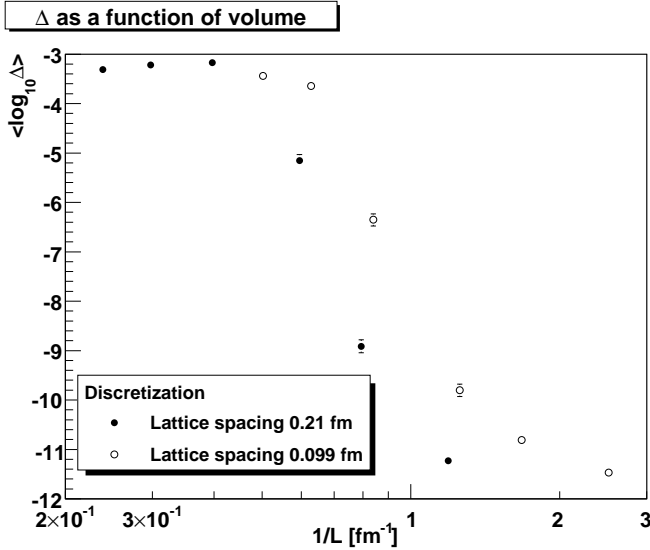


FIG. 15: The presence of Gribov copies as measured by  $\Delta$  as a function of inverse volume in four dimensions. Full circles correspond to  $\beta = 2.2$ , while open circles correspond to  $\beta = 2.45$ .

likely that the results obtained so far for vertices in lattice calculations [48, 49, 50, 54, 55] will also not change significantly, given the volumes available so far for them, although this will require explicit verification [67]. Therefore, the correlation functions in the absolute Landau gauge seem to be in good agreement with the results from the GZKO scenario. This permits now to compare the results from functional (Dyson-Schwinger) calculations and lattice calculations with some confidence in the three-dimensional case. This is shown in figure 16. The agreement is rather good.

There are still two more issues.

The reason for the interesting non-smooth behavior of the ghost propagator shown in figure 12 in three dimensions may be connected to the volume evolution of the first Gribov region and the fundamental modular region. Due to volume effects, in both cases configurations at the boundary dominate the average. However, at any finite volume both do not have a common boundary [5, 6]. Given that the first Gribov region is bounded by configurations with the smallest eigenvalues of the Faddeev-Popov operator, the ghost propagator has to diverge less in absolute Landau gauge than in minimal Landau gauge for small volumes. Furthermore, with the ghost propagator different in both gauges, this implies that the Faddeev-Popov operator eigenspectrum on the common boundary must be differently shaped than on the non-common boundary<sup>10</sup>. Only when both bound-

<sup>10</sup> Note that a large part of the low-lying Faddeev-Popov operator eigenspectrum influences the low-momentum part of the ghost propagator [72].

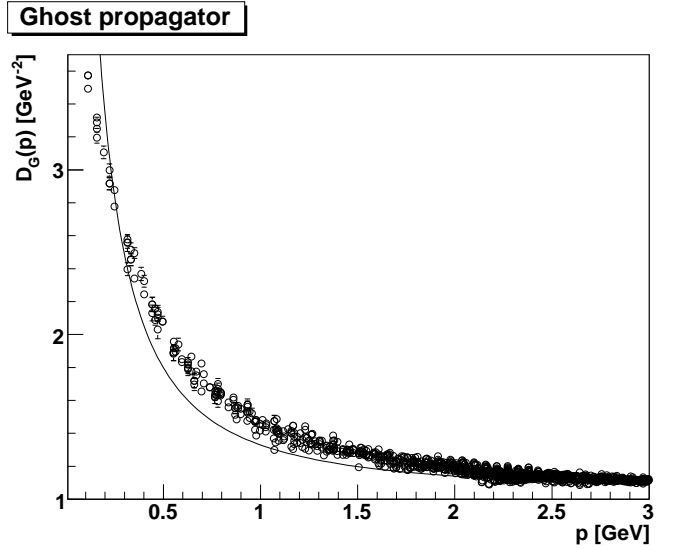
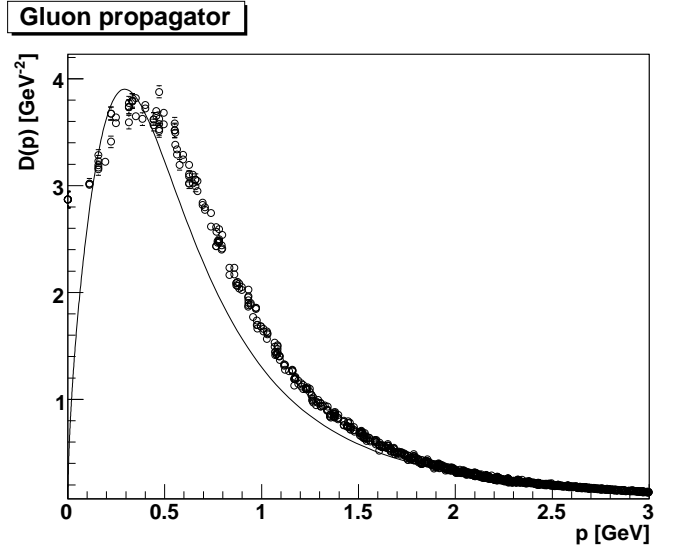


FIG. 16: The lattice results in absolute Landau gauge from a  $64^3$  lattice at  $\beta = 4.24$  compared to results from DSE calculations [20].

aries approach each other with increasing volume, the latter effect can become dominant and the ghost propagator in absolute Landau gauge can be more divergent than in minimal Landau gauge. However, this reasoning is rather speculative.

Of course, the open question remains, why the conjecture [4] derived from the GZKO scenario that the results in the minimal and the absolute Landau gauge should start to coincide at sufficiently large volumes is apparently not correct. A possibility is that volumes far beyond the present reach are necessary, or that discretization artifacts are important in the minimal Landau

gauge<sup>11</sup> [64]. It is well possible that gauge-fixing may be affected by finite size effects. E. g., for Feynman gauge this is already the case at the perturbative level [73] and becomes even more problematic at the non-perturbative level [74].

## VI. SUMMARY

When performing gauge-fixed calculations in the non-perturbative regime, it is necessary to precisely specify how to treat the residual gauge orbit which exists due to Gribov-Singer copies. In particular, gauge-dependent correlation functions like propagators can depend on how the residual gauge orbit is treated.

The results here show that this is indeed the case when comparing the propagators in the minimal Landau gauge and the absolute Landau gauge. The differences quickly diminish with momenta, and are quantitatively essentially irrelevant at momenta larger than 1 GeV. However, in the far infrared region they lead to qualitatively different behaviors: In the absolute Landau gauge the gluon propagator is infrared vanishing and the ghost propagator is infrared enhanced compared to the one of a massless particle. Therefore the predictions from functional calculations and the Gribov-Zwanziger/Kugo-Ojima scenarios are qualitatively confirmed, at least in three and two dimensions.

It has furthermore been shown that the differences increase with volume and with the number of dimensions. It can therefore be expected that a similar result will also be found in four dimensions, once sufficient computational resources are available to treat the quantitatively much more severe problem of differentiating between both gauges. Hence a critical behavior of correlation functions in the far infrared in the absolute Landau gauge seems to exist. However, more computational resources, which then can also be used to address the question of possible discretization artifacts affecting the Zwanziger conjecture, will be necessary to establish a final and firm conclusion. Still, with the results obtained here, there are only a few possibilities left for doubt on the far infrared behavior of propagators. For any solution different from the scaling solution to be established, a very concise discussion of the precise gauge in which it was obtained and in which way it is affected by the condition (4) will be necessary.

## Acknowledgments

I am grateful to R. Alkofer, A. Cucchieri, C. S. Fischer, H. Gies, T. Mendes, J. M. Pawłowski and L. von Smekal

for helpful discussions. This work was supported by the DFG under grant number MA 3935/1-2 and by the FWF under grant number P20330. Part of the computing time was provided by the Slovak Grant Agency for Science, grant VEGA No. 2/6068/2006, and by the Helmholtz association, grant No. VH-NG-332 (Helmholtz Young Investigator group “Nonperturbative Phenomena in QCD”). I am indebted to C. S. Fischer and J. M. Pawłowski for a critical reading of the manuscript and helpful comments. The ROOT framework [75] has been used in this project.

## APPENDIX A: TECHNICAL DETAILS OF THE LATTICE SIMULATIONS

The configurations have been obtained using a hybrid heat-bath overrelaxation procedure using a standard Wilson action. Details of this procedure and the determination of the propagators along with statistical error determination procedures can be found in [55].

In total, three sets of data have been obtained. One set has been used in section III to investigate properties of the adaptive stochastic overrelaxation gauge-fixing procedure [55], which is used as an element in the method to fix to the absolute Landau gauge described in the next appendix B. The details of these simulations can be found in table I. In this set of data, the gauge-fixing procedure was limited in the number of iterations, as described in section III. For each limit, an independent set of configurations was used, to reduce systematic errors.

Note that for all data sets in tables I-VI multiple independent runs were always performed to reduce auto-correlation effects. In case of the largest volumes, usually less than ten configurations constitute an independent run.

A second set is obtained and fixed to the minimal Landau gauge using adaptive stochastic overrelaxation [55]. In this case, a random gauge transformation is used to initialize the iterative procedure. The results from these configurations are used for comparison between the minimal Landau gauge and the absolute Landau gauge in section IV. The details of these configurations are listed in table II in two dimensions and in table III in three dimensions. The number of configurations was tuned to obtain the exponent of the ghost propagator with a statistical accuracy of better than 10% at the  $1\sigma$ -level.

The third set contains the configurations which have been fixed to the absolute Landau gauge. Details on these can be found for two dimensions in table IV, in table V for three dimensions, and in table VI for four dimensions. Note that in this case it was not always possible to achieve the desired statistical accuracy, as it took, for the largest volume, up to one CPU-week on a current standard processor to obtain one gauge-fixed configuration. The final statistical accuracy achieved was the best obtainable with the available resources. Additional information concerning the gauge-fixing procedure is provided

---

<sup>11</sup> This is also possible in case of the absolute Landau gauge, although so far no indications for this have been found.

TABLE I: Number of configurations considered in the numerical simulations for the results of section III. The value of the lattice spacing  $a$  has been taken from Ref. [51]. All calculations have been performed in three dimensions on a  $40^3$  lattice at  $\beta = 4.2$ . Always 200 thermalization sweeps and 50 sweeps between two consecutive measurements have been performed. 'Limit' is the maximum number of permitted gauge fixing sweeps, and 'Conf.' the number of configurations used. The limit  $\infty$  corresponds to no restriction on the number of gauge-fixing sweeps, and the number in parentheses is the actual maximum number observed. The data in this case is taken from [50], and the first and second number of configurations refers to the number of configurations used for the ghost and gluon propagator, respectively. Note that for each limit case independent configurations have been obtained. Note further that in all cases multiple independent runs (about 15-20) have been performed to obtain the data.

Limit	Conf.	Limit	Conf.	Limit	Conf.
$\infty$ (28740)	1077/8175	27303	1091	25938	1262
24641	1030	23409	1021	22239	1029
21127	1016	20071	1060	19067	1148
18114	1043	17208	1088	16348	1150
15531	1080	14754	1083	14016	1004
13315	1154	12649	1125	12017	1106
11416	1135	10845	1032	10303	1032
9788	1128	9299	1134	8834	1154
8392	1154	7972	1050	7573	1154
7195	1154	6835	1131	6493	1184
6168	1131	5860	1213	5567	1088
5289	1116	5025	1161	4773	1047
4535	1237	4308	1150	4093	1131
3888	1128	3694	1138	3509	1136
3334	1158	3167	1131	3009	1154
2858	1154	2715	1048	2579	1112
2450	1111	2328	1113	2212	1103
2101	1078	1996	1061	1896	1153
1801	1153	1711	967	1626	967
1545	986	1467	1026	1394	991
1324	1088	1258	853	1195	752
1135	593	1078	1136	1024	854
972	666	923	554	876	781
832	407	791	632	751	366
714	80	678	196	644	148

in the tables IV-VI. The description of these can be found in the next appendix B on the gauge-fixing algorithm.

## APPENDIX B: FIXING TO THE ABSOLUTE LANDAU GAUGE

Fixing to the absolute Landau gauge as specified in section II is a hard problem. Actually it is NP-hard, similar to finding the ground state of a spin glass Hamiltonian, to the best of current knowledge. Therefore, there is no hope to really find the absolute minimum of (3). In particular, confirming to have found the absolute minimum of (3) is in itself a problem at least as hard as

TABLE II: Number of configurations considered in the numerical simulations for the results in minimal Landau gauge of section IV in two dimensions. The value of the lattice spacing  $a$  has been determined analytically [76]. To assign units the standard value of  $(440 \text{ MeV})^2$  has been assigned to the string tension.  $N$  is the number of lattice sites in one direction of the symmetric lattice,  $a$  is the lattice spacing,  $L$  the physical length extent, 'Therm.' the number of thermalization sweeps, 'Sweep' the number of sweeps between two consecutive measurements and 'Conf.' the total number of configurations. Note that in all cases multiple independent runs have been performed to obtain the data.

$N$	$\beta$	$a$ [fm]	$a^{-1}$ [GeV]	$L$ [fm]	Therm.	Sweep	Conf.
4	38.7	0.089	2.2	0.36	140	14	1045
4	10	0.18	1.1	0.72	140	14	1045
10	38.7	0.089	2.2	0.89	200	20	1589
16	38.7	0.089	2.2	1.4	260	26	1017
10	10	0.18	1.1	1.8	200	20	2365
20	38.7	0.089	2.2	1.8	300	30	1094
26	38.7	0.089	2.2	2.3	360	36	1015
16	10	0.18	1.1	2.9	260	26	1017
34	38.7	0.089	2.2	3.0	440	44	1038
20	10	0.18	1.1	3.6	300	30	1041
44	38.7	0.089	2.2	3.9	540	54	1060
26	10	0.18	1.1	4.7	360	36	1009
56	38.7	0.089	2.2	5.0	660	66	1054
34	10	0.18	1.1	6.1	440	44	1038
68	38.7	0.089	2.2	6.1	680	68	1011
80	38.7	0.089	2.2	7.1	900	90	1113
44	10	0.18	1.1	7.9	540	54	1059
104	38.7	0.089	2.2	9.3	1140	114	1045
56	10	0.18	1.1	10	660	66	6564
112	38.7	0.089	2.2	10	1220	122	3524
68	10	0.18	1.1	12	780	78	1011
136	38.7	0.089	2.2	12	1460	146	2179
150	38.7	0.089	2.2	13	1600	160	1066
80	10	0.18	1.1	14	900	90	1048
166	38.7	0.089	2.2	15	1760	176	916
184	38.7	0.089	2.2	16	1940	194	130
104	10	0.18	1.1	19	1140	114	1032
112	10	0.18	1.1	20	1220	122	2250
136	10	0.18	1.1	25	1460	146	1981
150	10	0.18	1.1	27	1600	160	2238
166	10	0.18	1.1	30	1760	176	1286
184	10	0.18	1.1	33	1940	194	201

the original problem of finding the minimum. Therefore, the best attempt, which is pursued here, is to improve the condition (4). That this at least resembles the absolute Landau gauge rests on the assumption that the evolution of all (relevant) quantities with the value of (3) is smooth, and the limit itself is also not discontinuous. Hence, by getting closer and closer to the absolute minimum the propagators should become more and more like the ones in the correct absolute Landau gauge. On the smallest lattices, there is a reasonable hope to have found the absolute minimum in most of the cases. There, no discontinuous behavior has been found, giving at least

TABLE III: Number of configurations considered in the numerical simulations for the results in minimal Landau gauge of section IV in three dimensions. The value of the lattice spacing  $a$  has been determined by interpolation from Ref. [51]. To assign units the standard value of  $(440 \text{ MeV})^2$  has been assigned to the string tension. For further details, see table II.

$N$	$\beta$	$a$ [fm]	$a^{-1}$ [GeV]	$L$ [fm]	Therm.	Sweep	Conf.
4	7.09	0.090	2.2	0.36	240	24	1070
4	4.24	0.17	1.1	0.68	240	24	1070
8	7.09	0.090	2.2	0.72	280	28	1133
12	7.09	0.090	2.2	1.1	320	32	1070
8	4.24	0.17	1.1	1.4	280	28	1070
16	7.09	0.090	2.2	1.4	360	36	1144
20	7.09	0.090	2.2	1.8	400	40	1100
12	4.24	0.17	1.1	2.0	320	32	1128
24	7.09	0.090	2.2	2.2	440	44	1084
16	4.24	0.17	1.1	2.7	360	36	1048
32	7.09	0.090	2.2	2.9	520	52	960
20	4.24	0.17	1.1	3.4	400	40	1217
40	7.09	0.090	2.2	3.6	600	60	1065
24	4.24	0.17	1.1	4.1	440	44	1238
48	7.09	0.090	2.2	4.3	680	68	1095
56	7.09	0.090	2.2	5.0	760	76	1078
32	4.24	0.17	1.1	5.4	520	52	899
64	7.09	0.090	2.2	5.8	840	84	1062
40	4.24	0.17	1.1	6.8	600	60	1040
48	4.24	0.17	1.1	8.2	680	68	1047
56	4.24	0.17	1.1	9.5	760	76	1053
64	4.24	0.17	1.1	11	840	84	1033

some justification for this assumption.

It is then necessary to design an algorithm which aims at improving the condition (3). This has often been pursued using multiple restart algorithms [52, 57], stimulated annealing [44] and other approaches [46, 58, 65, 66]. However, the problem of gauge-fixing is, as has been discussed in section III, highly configuration-dependent. It is therefore desirable to use an algorithm which is able to adapt to a given configuration. One possibility are genetic (or evolutionary) algorithms [68]. This type of algorithms has been used previously for gauge-fixing in lattice gauge theory [58, 65, 66]. Here, a different flavor of such an algorithm is constructed and used throughout section IV.

The following algorithm has been performed for any given configuration  $\mathcal{C}$ :

- 1) Generate an initial population of  $N_W$  gauge transformations. They are obtained using an adaptive stochastic overrelaxation algorithm from once the identity transformation and  $N_W - 1$  random gauge transformations, and all fix  $\mathcal{C}$  to the Landau gauge<sup>12</sup>

- 2) Determine the fitness of each member of the population by calculating (3) for it
- 3) Remove the  $N_W/2$  elements with the lowest fitness function, obtaining the parent generation  $\mathcal{P}$ . Note that all digits of the fitness function are always considered, i. e., even two members with a fitness only differing by machine precision fluctuations are not considered equal. Then construct a new generation by the following operations

- a) Generate  $0.15N_W = N_p$  new members by point mutation<sup>13</sup>. For this, select one member from  $\mathcal{P}$  randomly. Then draw a random number  $R$  according to a Gaussian distribution with a given width  $P_p$ . Take the absolute value, and if the number is smaller than 1 set it to one. Replace at  $R$  randomly chosen lattice points  $x$  the local gauge transformation matrix  $g(x)$  by a randomly chosen SU(2) matrix. Permit multiple replacements. However,  $P_p$  should be chosen sufficiently small. Here, it was selected to be 1% of the number of lattice sites. Use the so generated initial gauge transformation as seeds to obtain once again a gauge transformation of  $\mathcal{C}$  to Landau gauge
- b) Generate  $0.2N_W = N_c$  new members by crossing. For this purpose select two different members from  $\mathcal{P}$  randomly. Then construct a new member by mixing these two parent members. For this, select at each lattice site randomly from which parent to take the matrix  $g(x)$ . Use this new member as a seed to obtain a gauge transformation of  $\mathcal{C}$  to Landau gauge
- c) Add an additional number  $N_m$  of new members such that the population again consists of  $N_W$  members. These are again randomly initialized gauge transformations, which are then used to construct gauge transformations of  $\mathcal{C}$  to Landau gauge

- 4) Determine the fitness of all members according to (3). If none of the new members are better than those of the set  $\mathcal{P}$ , terminate the algorithm and use the fittest member for the gauge transformation to absolute Landau gauge. If a better new member exists, go to point 3 and repeat until the termination criterion is satisfied. A new member is also considered better if it only differs from the best so far in fitness by an amount of the order of the machine precision

<sup>12</sup> reached by using adaptive stochastic overrelaxation [55].

<sup>13</sup> Non-integer numbers are always rounded mathematically, but set to one if zero.

<sup>12</sup> Landau gauge refers here to the (local) minimum of (3) which is

TABLE IV: Number of configurations considered in the numerical simulations for the results in absolute Landau gauge of section IV in two dimensions. For details see table II. The additional parameters  $N_w$ ,  $N_p$ ,  $P_p$ ,  $N_c$ ,  $N_m$  are explained in appendix B.  $N_g$  is the average number of generations,  $N_x$  the maximum number of generations, and  $N_{\min}$ ,  $N_f$ , and  $N_{\max}$  are the minimum number, the average number per configuration, and the maximally needed number of gauge-fixings, respectively.

$N$	$\beta$	$a$ [fm]	$a^{-1}$ [GeV]	$L$ [fm]	Therm.	Sweep	Conf.	$N_W$	$N_p$	$P_p$	$N_c$	$N_m$	$N_g$	$N_x$	$N_{\min}$	$N_f$	$N_{\max}$
4	38.7	0.089	2.2	0.36	140	14	1027	8	1	0.16	1	2	2.36(2)	6	12	13.44(8)	28
4	10	0.18	1.1	0.72	140	14	1027	8	1	0.16	1	2	2.76(3)	6	12	15.0(1)	28
10	38.7	0.089	2.2	0.89	200	20	1208	10	1	1.0	2	2	2.55(2)	9	15	17.8(1)	50
16	38.7	0.089	2.2	1.4	260	26	1049	12	1	2.6	2	3	2.58(2)	7	18	21.5(1)	48
10	10	0.18	1.1	1.8	200	20	1027	10	1	1.0	2	2	2.65(3)	8	15	18.3(2)	45
20	38.7	0.089	2.2	1.8	300	30	1041	14	2	4.0	2	3	2.75(3)	7	21	26.3(2)	56
26	38.7	0.089	2.2	2.3	360	36	1130	16	2	6.8	3	3	2.53(2)	8	24	28.2(2)	72
16	10	0.18	1.1	2.9	260	26	1037	12	1	2.6	2	3	2.53(2)	6	18	21.2(2)	42
34	38.7	0.089	2.2	3.0	440	44	1032	18	2	12	3	4	2.71(3)	7	27	33.4(8)	70
20	10	0.18	1.1	3.6	300	30	1119	14	2	4.0	2	3	2.63(2)	7	21	25.4(2)	56
44	38.7	0.089	2.2	3.9	540	54	1061	20	3	19	4	3	2.59(3)	7	30	35.9(3)	80
26	10	0.18	1.1	4.7	360	36	1065	16	2	6.8	3	3	2.59(3)	6	24	28.7(2)	56
56	38.7	0.089	2.2	5.0	660	66	1045	24	3	31	4	5	2.63(3)	7	36	43.6(4)	96
34	10	0.18	1.1	6.1	440	44	1032	18	2	12	3	4	2.55(3)	7	27	32.0(3)	70
68	38.7	0.089	2.2	6.1	680	68	1130	28	4	46	5	5	2.47(2)	6	42	48.6(3)	98
80	38.7	0.089	2.2	7.1	900	90	1084	32	4	64	6	6	2.52(2)	6	48	56.3(3)	112
44	10	0.18	1.1	7.9	540	54	1006	20	3	19	4	3	2.46(2)	6	30	34.6(2)	70
104	38.7	0.089	2.2	9.3	1140	114	2078	36	5	108	7	6	2.50(2)	7	54	63.0(4)	144
56	10	0.18	1.1	10	660	66	1083	24	3	31	4	5	2.56(2)	7	36	42.7(2)	96
112	38.7	0.089	2.2	10	1220	122	1068	40	6	125	8	6	2.50(3)	7	60	70.0(6)	160
68	10	0.18	1.1	12	780	78	1014	28	4	46	5	5	2.47(2)	6	42	48.6(3)	98
136	38.7	0.089	2.2	12	1460	146	1028	46	6	185	9	8	2.49(2)	7	69	80.3(5)	184
150	38.7	0.089	2.2	13	1600	160	459	52	7	225	10	9	2.49(3)	6	78	90.7(8)	182
80	10	0.18	1.1	14	900	90	2136	32	4	64	6	6	2.45(2)	8	48	55.2(3)	144
166	38.7	0.089	2.2	15	1760	176	326	58	8	276	11	10	2.52(5)	6	87	102(1)	203
184	38.7	0.089	2.2	16	1940	194	66	64	9	339	12	11	2.45(9)	5	96	110(3)	192
104	10	0.18	1.1	19	1140	114	1096	36	5	108	7	6	2.44(2)	6	54	61.9(4)	126
112	10	0.18	1.1	20	1220	122	2105	40	6	125	8	6	2.45(2)	10	60	69.0(4)	220
136	10	0.18	1.1	24	1460	146	1414	46	6	185	9	8	2.46(2)	7	69	79.6(5)	184
150	10	0.18	1.1	27	1600	160	748	52	7	225	10	9	2.51(3)	7	78	91.3(8)	208
166	10	0.18	1.1	30	1760	176	267	58	8	276	11	10	2.52(6)	6	87	102(2)	203
184	10	0.18	1.1	33	1940	194	53	64	9	339	12	11	2.36(8)	4	96	108(3)	160

Note that this algorithm does not guarantee to terminate after a number of generations. However, in practice it always terminates. In most cases, already the second generation did not yield any improvement, but the maximum number of generations  $N_x$  has been as large as 10 for the systems investigated here. The average number of generations  $N_g$  is always between two and a bit more than three, yielding therefore a total number of performed gauge-fixings between  $3/2N_W$  and roughly  $2N_W$ . Given that the number of Gribov copies grows exponentially with the number of lattice sites,  $N_W$  also has to grow with the number of lattice sites. Strict exponential growth is at this time prohibited by computational resources. The values chosen in practice are listed in ta-

bles IV-VI.

Note that the numbers  $N_W$ ,  $N_p$ ,  $N_c$ ,  $N_m$ , and  $P_p$  are far from optimized, and result only from experiments on small lattices. This algorithm can and should be improved, if fixing to the absolute Landau gauge turns out to be important for applications. Furthermore, the structure of the algorithm is itself subject to optimization, and may possibly be more efficient if other structures were admitted as well [68]. Finally, there exists some knowledge on the structure of Gribov copies [78]. In particular, they exhibit a domain-like structure. Incorporating this prior knowledge in, e. g., the crossing of two gauge transformations may furthermore improve the efficiency of the algorithm.

[1] R. J. Rivers, "Path integral methods in quantum field theory," *Cambridge, UK: Univ. Pr. (1987) 339 p. (Cam-*

*bridge monographs on mathematical physics).*

[2] M. Bohm, A. Denner and H. Joos, "Gauge Theories

TABLE V: Number of configurations considered in the numerical simulations for the results in absolute Landau gauge of section IV in three dimensions. See table III and IV as well as appendix B for details.

$N$	$\beta$	$a$ [fm]	$a^{-1}$ [GeV]	$L$ [fm]	Therm.	Sweep	Conf.	$N_W$	$N_p$	$P_p$	$N_c$	$N_m$	$N_g$	$N_x$	$N_{\min}$	$N_f$	$N_{\max}$
4	7.09	0.090	2.2	0.36	240	24	1092	8	1	0.64	1	2	2.70(2)	6	12	14.8(2)	28
4	4.24	0.17	1.1	0.68	240	24	1270	8	1	0.64	1	2	2.67(2)	7	12	14.7(2)	32
8	7.09	0.090	2.2	0.72	280	28	1115	10	1	5.1	2	2	2.69(3)	9	15	18.5(2)	50
12	7.09	0.090	2.2	1.1	320	32	1115	12	1	17	2	3	2.68(3)	7	18	22.1(2)	48
8	4.24	0.17	1.1	1.4	280	28	1196	10	1	5.1	2	2	2.73(3)	7	15	18.7(2)	40
16	7.09	0.090	2.2	1.4	360	36	1106	14	2	41	2	3	2.62(3)	8	21	25.3(2)	63
20	7.09	0.090	2.2	1.8	400	40	1144	16	2	80	3	3	2.64(2)	8	24	29.1(2)	72
12	4.24	0.17	1.1	2.0	320	32	1109	12	1	17	2	3	2.54(2)	6	18	21.2(1)	42
24	7.09	0.090	2.2	2.2	440	44	1093	18	2	138	3	4	2.56(3)	7	27	32.0(3)	72
16	4.24	0.17	1.1	2.7	360	36	1041	14	2	41	2	3	2.54(3)	8	21	24.8(2)	63
32	7.09	0.090	2.2	2.9	520	52	1025	20	3	328	4	3	2.68(3)	8	30	36.8(3)	90
20	4.24	0.17	1.1	3.4	400	40	1302	16	2	80	3	3	2.60(3)	8	24	28.8(2)	72
40	7.09	0.090	2.2	3.6	600	60	1005	24	3	640	4	5	2.73(3)	8	36	44.8(4)	108
24	4.24	0.17	1.1	4.1	440	44	1095	18	2	138	3	4	2.57(3)	7	27	32.1(3)	72
48	7.09	0.090	2.2	4.3	680	68	906	28	4	1106	5	5	2.84(3)	8	42	53.8(4)	126
56	7.09	0.090	2.2	5.0	760	76	657	32	4	1756	6	6	2.83(4)	8	48	61.3(6)	144
32	4.24	0.17	1.1	5.4	520	52	1072	20	3	328	4	3	2.71(3)	9	30	37.1(3)	100
64	7.09	0.090	2.2	5.8	840	84	167	36	5	2621	7	6	3.02(7)	6	54	72(1)	126
40	4.24	0.17	1.1	6.8	600	60	1026	24	3	640	4	5	2.72(3)	7	36	44.6(4)	96
48	4.24	0.17	1.1	8.2	680	68	929	28	4	1106	5	5	2.86(3)	8	42	54.0(4)	126
56	4.24	0.17	1.1	9.5	760	76	522	32	4	1756	6	6	2.87(4)	7	48	61.9(6)	128
64	4.24	0.17	1.1	11	840	84	291	36	5	2621	7	6	3.07(6)	7	54	73(1)	144

TABLE VI: Number of configurations considered in the numerical simulations for the results in absolute Landau gauge of section IV in four dimensions. See table III and IV as well as section B for details. The scale has been fixed according to [77].

$N$	$\beta$	$a$ [fm]	$a^{-1}$ [GeV]	$L$ [fm]	Therm.	Sweep	Conf.	$N_W$	$N_p$	$P_p$	$N_c$	$N_m$	$N_g$	$N_x$	$N_{\min}$	$N_f$	$N_{\max}$
4	2.45	0.099	2.0	0.40	340	34	1020	8	1	2.6	1	2	2.63(3)	7	12	14.5(1)	32
6	2.45	0.099	2.0	0.59	360	36	1191	10	1	13	2	2	2.60(3)	7	15	18.0(2)	40
8	2.45	0.099	2.0	0.79	380	38	1013	12	1	41	2	3	2.59(2)	8	18	21.5(1)	56
4	2.2	0.21	0.94	0.84	340	34	1132	8	1	2.6	1	2	2.63(2)	7	12	14.5(1)	32
12	2.45	0.099	2.0	1.2	420	42	1091	14	2	207	2	3	2.64(3)	9	21	25.5(2)	70
6	2.2	0.21	0.94	1.3	360	36	1191	10	1	13	2	2	2.57(3)	8	15	17.9(2)	45
16	2.45	0.099	2.0	1.6	460	46	652	16	2	655	3	3	2.65(4)	8	24	29.2(3)	72
8	2.2	0.21	0.94	1.7	380	38	1013	12	1	41	2	3	2.56(3)	6	18	21.4(2)	56
20	2.45	0.099	2.0	2.0	500	50	148	18	2	1600	3	4	2.72(9)	10	27	33.5(7)	100
12	2.2	0.099	0.94	2.5	420	42	1081	14	2	207	2	3	2.65(3)	7	21	25.6(2)	56
16	2.2	0.21	0.94	3.4	460	46	277	16	2	655	3	3	2.78(6)	8	24	30.2(5)	72
20	2.2	0.21	0.94	4.2	500	50	59	18	2	1600	3	4	2.7(1)	5	27	33.3(8)	54

- Of The Strong And Electroweak Interaction”, (Teubner, Stuttgart, 2001) 784 p.
- [3] V. N. Gribov, Nucl. Phys. B **139**, 1 (1978).
- [4] D. Zwanziger, Phys. Rev. D **69**, 016002 (2004) [arXiv: hep-ph/0303028].
- [5] D. Zwanziger, Phys. Rev. D **65**, 094039 (2002) [arXiv: hep-th/0109224]; Phys. Rev. D **67**, 105001 (2003) [arXiv: hep-th/0206053].
- [6] D. Zwanziger, Phys. Lett. B **257**, 168 (1991); Nucl. Phys. B **364**, 127 (1991); Nucl. Phys. B **412**, 657 (1994); Phys. Rev. D **65**, 094039 (2002) [arXiv: hep-th/0109224];
- [7] T. Kugo and I. Ojima, Prog. Theor. Phys. Suppl. **66**, 1 (1979) [Erratum Prog. Theor. Phys. **71**, 1121 (1984)]; T. Kugo, arXiv:hep-th/9511033.
- [8] L. von Smekal, A. Hauck and R. Alkofer, Annals Phys. **267** (1998) 1 [Erratum-ibid. **269** (1998) 182] [arXiv:hep-ph/9707327].
- [9] R. Alkofer and L. von Smekal, Phys. Rept. **353** (2001) 281 [arXiv:hep-ph/0007355].
- [10] P. Watson and R. Alkofer, PRL **86** (2001) 5239 [hep-ph/0102332].
- [11] C. Lerche and L. von Smekal, Phys. Rev. D **65**, 125006 (2002) [arXiv:hep-ph/0202194].
- [12] C. S. Fischer and R. Alkofer, Phys. Lett. B **536** (2002) 177 [arXiv:hep-ph/0202202]; C. S. Fischer, R. Alkofer and H. Reinhardt, Phys. Rev. D **65** (2002) 094008 [arXiv:hep-ph/0202195].
- [13] R. Alkofer, C. S. Fischer and F. J. Llanes-Estrada, Phys.

- Lett. B **611**, 279 (2005) [arXiv:hep-th/0412330].
- [14] W. Schleifenbaum, A. Maas, J. Wambach and R. Alkofer, Phys. Rev. D **72**, 014017 (2005) [arXiv:hep-ph/0411052].
- [15] C. S. Fischer, J. Phys. G **32**, R253 (2006) [arXiv:hep-ph/0605173].
- [16] C. S. Fischer and J. M. Pawłowski, Phys. Rev. D **75**, 025012 (2007) [arXiv:hep-th/0609009].
- [17] R. Alkofer, M. Q. Huber and K. Schwenzer, arXiv:0801.2762 [hep-th].
- [18] C. Kellermann and C. S. Fischer, Phys. Rev. D **78**, 025015 (2008) [arXiv:0801.2697 [hep-ph]].
- [19] M. Q. Huber, R. Alkofer, C. S. Fischer and K. Schwenzer, Phys. Lett. B **659** (2008) 434 [arXiv:0705.3809 [hep-ph]].
- [20] A. Maas, J. Wambach, B. Grüter and R. Alkofer, Eur. Phys. J. **C37**, No.3, 335 (2004) [arXiv:hep-ph/0408074].
- [21] A. C. Aguilar and A. A. Natale, JHEP **0408**, 057 (2004).
- [22] A. C. Aguilar and J. Papavassiliou, Phys. Rev. D **77**, 125022 (2008) [arXiv:0712.0780 [hep-ph]].
- [23] D. Binosi and J. Papavassiliou, Phys. Rev. D **77** (2008) 061702 [arXiv:0712.2707 [hep-ph]].
- [24] A. C. Aguilar, D. Binosi and J. Papavassiliou, arXiv:0802.1870 [hep-ph].
- [25] Ph. Boucaud, Th. Bruntjen, J. P. Leroy, A. Le Yaouanc, A. Y. Lokhov, J. Micheli, O. Pene and J. Rodriguez-Quintero, JHEP **0606**, 001 (2006) [arXiv:hep-ph/0604056].
- [26] Ph. Boucaud, J. P. Leroy, A. L. Yaouanc, J. Micheli, O. Pene and J. Rodriguez-Quintero, JHEP **0806**, 012 (2008) [arXiv:0801.2721 [hep-ph]].
- [27] Ph. Boucaud, J. P. Leroy, A. Le Yaouanc, J. Micheli, O. Pene and J. Rodriguez-Quintero, JHEP **0806**, 099 (2008) [arXiv:0803.2161 [hep-ph]].
- [28] J. C. R. Bloch, Phys. Rev. D **66** (2002) 034032 [arXiv:hep-ph/0202073].
- [29] C. S. Fischer, A. Maas, J. M. Pawłowski, to be published.
- [30] J. M. Pawłowski, D. F. Litim, S. Nedelko and L. von Smekal, Phys. Rev. Lett. **93** (2004) 152002 [arXiv:hep-th/0312324].
- [31] C. S. Fischer and H. Gies, JHEP **0410**, 048 (2004) [arXiv:hep-ph/0408089].
- [32] J. Braun, H. Gies and J. M. Pawłowski, arXiv:0708.2413 [hep-th].
- [33] D. Dudal, R. F. Sobreiro, S. P. Sorella and H. Verschelde, Phys. Rev. D **72**, 014016 (2005) [arXiv:hep-th/0502183].
- [34] D. Dudal, S. P. Sorella, N. Vandersickel and H. Verschelde, Phys. Rev. D **77**, 071501 (2008) [arXiv:0711.4496 [hep-th]].
- [35] M. A. L. Capri, D. Dudal, V. E. R. Lemes, R. F. Sobreiro, S. P. Sorella, R. Thibes and H. Verschelde, Eur. Phys. J. C **52**, 459 (2007) [arXiv:0705.3591 [hep-th]].
- [36] D. Dudal, J. Gracey, S. P. Sorella, N. Vandersickel and H. Verschelde, arXiv:0806.4348 [hep-th].
- [37] D. Dudal, J. A. Gracey, S. P. Sorella, N. Vandersickel and H. Verschelde, arXiv:0808.0893 [hep-th].
- [38] O. Oliveira and P. J. Silva, arXiv:0705.0964 [hep-lat].
- [39] J. C. R. Bloch, A. Cucchieri, K. Langfeld and T. Mendes, Nucl. Phys. B **687**, 76 (2004) [arXiv:hep-lat/0312036].
- [40] A. Sternbeck, E. M. Ilgenfritz, M. Mueller-Preussker and A. Schiller, Phys. Rev. D **72**, 014507 (2005) [arXiv:hep-lat/0506007].
- [41] A. Sternbeck, E. M. Ilgenfritz, M. Muller-Preussker, A. Schiller and I. L. Bogolubsky, PoS **LAT2006**, 076 (2006) [arXiv:hep-lat/0610053].
- [42] A. Cucchieri and T. Mendes, Braz. J. Phys. **37**, 484 (2007).
- [43] I. L. Bogolubsky, E. M. Ilgenfritz, M. Muller-Preussker and A. Sternbeck, PoS (LATTICE-2007) 290, arXiv:0710.1968 [hep-lat]; A. Cucchieri and T. Mendes, PoS (LATTICE 2007) 297, arXiv:0710.0412 [hep-lat].
- [44] A. Sternbeck, L. von Smekal, D. B. Leinweber and A. G. Williams, PoS (LATTICE 2007) 340, arXiv:0710.1982 [hep-lat].
- [45] A. Cucchieri and T. Mendes, Phys. Rev. Lett. **100**, 241601 (2008) [arXiv:0712.3517 [hep-lat]].
- [46] I. L. Bogolubsky, G. Burgio, M. Muller-Preussker and V. K. Mitrjushkin, Phys. Rev. D **74**, 034503 (2006) [arXiv:hep-lat/0511056]; I. L. Bogolubsky *et al.*, Phys. Rev. D **77**, 014504 (2008) [Erratum-ibid. D **77**, 039902 (2008)] [arXiv:0707.3611 [hep-lat]].
- [47] A. Cucchieri and T. Mendes, arXiv:0804.2371 [hep-lat].
- [48] C. Parrinello, Phys. Rev. D **50** (1994) 4247, [arXiv:hep-lat/9405024]; P. Boucaud, J. P. Leroy, J. Micheli, O. Pene and C. Roiesnel, JHEP **9810**, 017 (1998), [arXiv:hep-ph/9810322].
- [49] E. M. Ilgenfritz, M. Muller-Preussker, A. Sternbeck, A. Schiller and I. L. Bogolubsky, Braz. J. Phys. **37**, 193 (2007) [arXiv:hep-lat/0609043].
- [50] A. Cucchieri, A. Maas and T. Mendes, Phys. Rev. D **77**, 094510 (2008) [arXiv:0803.1798 [hep-lat]].
- [51] A. Cucchieri, T. Mendes and A. R. Taurines, Phys. Rev. D **67**, 091502 (2003) [arXiv:hep-lat/0302022].
- [52] A. Cucchieri, Nucl. Phys. B **521**, 365 (1998) [arXiv:hep-lat/9711024].
- [53] A. Cucchieri, A. Maas and T. Mendes, Phys. Rev. D **75** (2007) 076003 [arXiv:hep-lat/0702022].
- [54] A. Maas, Phys. Rev. D **75**, 116004 (2007) [arXiv:0704.0722 [hep-lat]].
- [55] A. Cucchieri, A. Maas and T. Mendes, Phys. Rev. D **74**, 014503 (2006) [arXiv:hep-lat/0605011].
- [56] C. S. Fischer, A. Maas, J. M. Pawłowski and L. von Smekal, Annals Phys. **322** (2007) 2916 [arXiv:hep-ph/0701050].
- [57] T. D. Bakeev, E. M. Ilgenfritz, V. K. Mitrjushkin and M. Mueller-Preussker, Phys. Rev. D **69** (2004) 074507 [arXiv:hep-lat/0311041].
- [58] P. J. Silva and O. Oliveira, Nucl. Phys. B **690**, 177 (2004) [arXiv:hep-lat/0403026].
- [59] I. M. Singer, Commun. Math. Phys. **60** (1978) 7.
- [60] A. Maas, Eur. Phys. J. C **48** (2006) 179 [arXiv:hep-th/0511307].
- [61] P. van Baal, arXiv:hep-th/9711070; M. Semenov-Tyan-Shanskii and V. Franke, Zap. Nauch. Sem. Leningrad. Otdeleniya Matematicheskogo Instituta in V. A. Stekolov, AN SSSR, Vol. 120 (1982), 159 (In English translation: New York, Plenum Press 1986); G. Dell'Antonio, D. Zwanziger, Proceedings of the NATO Advanced Workshop on Probabilistic Methods in Quantum Field Theory and Quantum Gravity, Cargese. New York, Plenum Press (1986), 21.
- [62] A. Cucchieri and T. Mendes, Nucl. Phys. B **471**, 263 (1996) [arXiv:hep-lat/9511020]; Nucl. Phys. Proc. Suppl. **53**, 811 (1997) [arXiv:hep-lat/9608051].
- [63] P. Hirschfeld, Nucl. Phys. B **157** (1979) 37; R. Friedberg, T. D. Lee, Y. Pang and H. C. Ren, Annals Phys. **246** (1996) 381.
- [64] L. von Smekal, talk at "Quarks and Hadrons in Strong QCD", St. Goar, Germany, March 2008.
- [65] O. Oliveira and P. J. Silva, Comput. Phys. Commun.

- 158**, 73 (2004) [arXiv:hep-lat/0309184].
- [66] A. Yamaguchi and A. Sugamoto, Nucl. Phys. Proc. Suppl. **83**, 837 (2000) [arXiv:hep-lat/9909063]; A. Yamaguchi and H. Nakajima, Nucl. Phys. Proc. Suppl. **83**, 840 (2000) [arXiv:hep-lat/9909064]; A. Yamaguchi, Nucl. Phys. Proc. Suppl. **73**, 847 (1999) [arXiv:hep-lat/9809068].
- [67] A. Maas, work in progress.
- [68] W. Banzhaf, P. Nordin, R. E. Keller, "Genetic Programming. An introduction.", Morgan Kaufman Publ. Inc. San Francisco (1998).
- [69] L. Giusti, M. L. Paciello, C. Parrinello, S. Petrarca and B. Taglienti, Int. J. Mod. Phys. A **16**, 3487 (2001) [arXiv:hep-lat/0104012].
- [70] A. Cucchieri, Phys. Rev. D **60**, 034508 (1999) [arXiv:hep-lat/9902023].
- [71] P. de Forcrand and J. E. Hetrick, Nucl. Phys. Proc. Suppl. **42**, 861 (1995) [arXiv:hep-lat/9412044].
- [72] A. Sternbeck, E. M. Ilgenfritz and M. Muller-Preussker, Phys. Rev. D **73**, 014502 (2006) [arXiv:hep-lat/0510109].
- [73] J. Rank, *Thermal Screening Masses in the Standard Model of Strong and Electroweak Interactions*, Ph.D. thesis, Bielefeld University, January 1998, <http://www.physik.uni-bielefeld.de/theory/e6/publiframe.html>.
- [74] A. Cucchieri, A. Maas and T. Mendes, arXiv:0806.3124 [hep-lat].
- [75] R. Brun and F. Rademakers, Nucl. Instrum. Meth. A **389** (1997) 81.
- [76] H. G. Dosch and V. F. Muller, Fortsch. Phys. **27**, 547 (1979).
- [77] E. Manousakis and J. Polonyi, Phys. Rev. Lett. **58** (1987) 847; G. S. Bali, J. Fingberg, U. M. Heller, F. Karsch and K. Schilling, Phys. Rev. Lett. **71** (1993) 3059 [arXiv:hep-lat/9306024].
- [78] T. Heinzl, K. Langfeld, M. Lavelle and D. McMullan, Phys. Rev. D **76**, 114510 (2007) [arXiv:0705.2718 [hep-lat]].